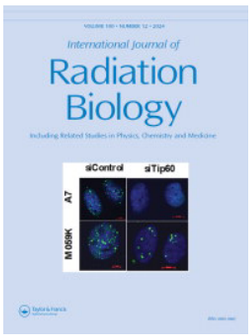

International Journal of Radiation Biology

ISSN: (Print) (Online) Journal homepage: www.tandfonline.com/journals/irab20

N-acetyl-L-tryptophan provides radioprotection to mouse and primate models by antagonizing the TRPV1 receptor and substance P inhibition

Raj Kumar, Pratibha Kumari, Neelanshu Gaurav, Ravi Kumar, Darshana Singh, Poonam Malhotra, Shravan Kumar Singh, Rabi Sankar Bhatta, Anil Kumar, Perumal Nagarajan, Surender Singh, Nishu Dalal, Bal Gangadhar Roy, Anant Narayan Bhatt & Sudhir Chandna

To cite this article: Raj Kumar, Pratibha Kumari, Neelanshu Gaurav, Ravi Kumar, Darshana Singh, Poonam Malhotra, Shravan Kumar Singh, Rabi Sankar Bhatta, Anil Kumar, Perumal Nagarajan, Surender Singh, Nishu Dalal, Bal Gangadhar Roy, Anant Narayan Bhatt & Sudhir Chandna (16 Dec 2024): N-acetyl-L-tryptophan provides radioprotection to mouse and primate models by antagonizing the TRPV1 receptor and substance P inhibition, International Journal of Radiation Biology, DOI: 10.1080/09553002.2024.2435330

To link to this article: https://doi.org/10.1080/09553002.2024.2435330

Published online: 16 Dec 2024.

INTERNATIONAL JOURNAL OF RADIATION BIOLOGY
https://doi.org/10.1080/09553002.2024.2435330

Taylor & Francis
Taylor & Francis Group

ORIGINAL ARTICLE

N-acetyl-L-tryptophan provides radioprotection to mouse and primate models by antagonizing the TRPV1 receptor and substance P inhibition

Raj Kumar[a], Pratibha Kumari[a], Neelanshu Gaurav[a], Ravi Kumar[a], Darshana Singh[a], Poonam Malhotra[a], Shravan Kumar Singh[a], Rabi Sankar Bhatta[b], Anil Kumar[c], Perumal Nagarajan[c], Surender Singh[c], Nishu Dalal[c], Bal Gangadhar Roy[a], Anant Narayan Bhatt[a] and Sudhir Chandna[a]

[a]Department of Radiation Biotechnology, Institute of Nuclear Medicine and Allied Sciences, Delhi, India; [b]Central Drug Research Institute (CDRI), Lucknow, India; [c]National Institute of Immunology (NII), Delhi

ABSTRACT

Purpose: The present study was carried out to evaluate the radioprotective activities of N-acetyl-L-tryptophan (L-NAT) using rodent and non-human primate (NHP) models.

Materials and methods: The antagonistic effect of L-NAT on the Transient receptor potential vanilloid-1 (TRPV1) receptor and substance P inhibition was determined using molecular docking and Elisa assays. The in *vivo* radioprotective activity of L-NAT was evaluated using whole-body survival assays in mice and NHPs. Radioprotective activity of L-NAT was also determined at the systemic level using quantitative histological analysis of bone marrow, jejunum, and seminiferous tubules of irradiated mice.

Results: Molecular docking studies revealed a strong binding of L-NAT with TRPV1 receptor at similar binding pockets to which capsaicin, an agonist of the TRPV1 receptor, binds. Further, capsaicin and gamma radiation were found to induce substance P levels in the intestines and serum of the mice, while L-NAT pretreatment was found to inhibit it. Significant whole-body survival (>80%) was observed in irradiated (9.0 Gy) mice that pretreated with L-NAT (150 mg/kg, b.wt. im) compared to 0% survival in irradiated mice that not pretreated with L-NAT. The quantitative histology of the hematopoietic, gastrointestinal, and male reproductive systems demonstrated significant protection against radiation-induced cellular degeneration. Interestingly, 100% survival was observed with irradiated NHPs (6.5 Gy) that pretreated with L-NAT (37.5 mg/kg, b.wt.im). Significant improvement in the hematology profile was observed after days 10-20 post-treatment periods in irradiated (6.5 Gy) NHPs that were pretreated with L-NAT.

Conclusion: L-NAT demonstrated excellent radioprotective activity in the mice and NHP models, probably by antagonizing TRPV1 receptor and subsequently inhibiting substance P expression.

ARTICLE HISTORY
Received 3 July 2024
Revised 8 November 2024
Accepted 14 November 2024

KEYWORDS
N-acetyl-L-tryptophan; radioprotection; acute radiation syndrome (ARS); efficacy biomarker; systemic radioprotection

Introduction

Ionizing radiation induces oxidative stress in the cellular milieu via radiolysis of cellular water, resulting in free radical generation. Free radicals interact with vital macromolecules like protein complexes, membrane lipids, DNA, and RNA *via* direct and indirect ways and oxidize them, resulting in irreversible oxidative damage. Gamma radiation exposure initiates various phenomena in the body, such as, redox imbalance, ionic disturbances, inflammation and cell death resulting in hematopoietic radiation syndrome (HRS), and gastro-intestinal radiation syndrome (GRS). Radiation induced systemic syndromes ultimately aggravated in the form of acute radiation syndrome (ARS). HRS is the primary phenomenon that may contribute to GRS and ARS based on the quantum of radiation dose absorbed in the biological tissues. Several incidences of accidental and deliberate radiation exposure have been reported in the past, compelling to develop radioprotectors and radiomitigators to manage radiation medical emergencies in the future. In response to the nuclear strikes on Hiroshima and Nagasaki, as well as other nuclear submarine mishaps and nuclear power plant accidents around the world, researchers from developed nations have launched multiple attempts to create radioprotectors. However, due to various unwanted side effects, toxicity, low time window and narrow therapeutic index etc., not a single radioprotective drug molecule has been approved by the US-FDA for human applications so far. First radioprotector i.e. WR-2721, developed by Walter Reed Research Institute, USA is still not achieved IND status for ARS indication due to its unacceptable toxicity at therapeutic dose in humans (Clement and Johnson 1982). Though, it has been approved for other indications such as radiation induced xerostomia and renal toxicity. Radiation countermeasure agents that achieved IND status in the USA are 5-AED, genistein, CBLB-502, Ex-Rad, Hema MaxTM

CONTACT Raj Kumar rajkumar.inmas@gov.in; rajkumar790@yahoo.com Department of Radiation Biotechnology, Institute of Nuclear Medicine and Allied Sciences (INMAS), Defence Research and Development Organization (DRDO), Delhi, India

(recombinant IL-12), Orbishield™ and G-CSF (Burdelya et al. 2008, 2012; Singh et al. 2014; 2015; Guan et al. 2023). Apart from that, Indralin (B-190) developed by Russian investigators, is also at an advanced stage of development (Vasin et al. 2014). However, no information about its emergency use approval is available. In the cellular environment, the most obvious criterion to screen radioprotectors is based on their antioxidant capacity. However, DNA repair enhancers (X-RAD), hematopoietic system modulator gamma tocotrienol, HL-003 and cell signaling modulators TLR5 agonist CBLB-502 are also being investigated and at advance stage of development (Burdelya et al. 2008; Kang et al. 2013; Obrador et al. 2020; Liu et al. 2021; Garg et al. 2022). Despite tremendous efforts worldwide, no FDA approval for radioprotectors was granted for human applications till date, possibly due to (i) non –uniformity in the efficacy levels among different animal species, (ii) un-acceptable toxicity of efficacious molecules at therapeutic doses, (iii) non-conformity in pharmaceutical actions, and (iv) identification and validation of efficacy biomarker(s) across the animals' species. Besides that, ethical issues associated with human efficacy trial of radioprotectors act as a prominent impediment in the efficacy conformity with human volunteers.

The present study was conducted to investigate radioprotective activities of N-acetyl-L-tryptophan (L-NAT) in the mice and non-human primate (NHP; Rhesus Macaque) models against lethal gamma radiation exposure. Whole body 30 days survival for the irradiated mice and 60 days survival for irradiated NHPs was considered as the end point of the study to decide the radioprotective efficacy of L-NAT. To evaluate the systemic radioprotection offered by L-NAT, quantitative histopathological analysis of hematopoietic, gastrointestinal and male reproductive systems was carried out using mice model. To determine the radioprotective efficacy of L-NAT in NHPs (Rhesus Macaque; both male and female) were used. To further strengthen the radioprotective potential of L-NAT in NHP model, comprehensive hematology, blood biochemistry, DNA damage and efficacy biomarker expression analysis was undertaken. To unravel the molecular mechanism of radioprotection offered by L-NAT, Transient receptor potential vanilloid-1 (TRPV1) receptor antagonistic and subsequent substance P expression inhibition studies was carried out using molecular docking tools and subsequent substance P expression analysis in the serum and intestine of irradiated and L-NAT treated mice.

Materials and methods

Materials

Ethanol was purchased from Merck India Pvt. Ltd, Mumbai, India. Disodium hydrogen phosphate (Na2HPO4.2H2O) and Dimethyl sulfoxide (DMSO) were purchased from Central Drug House, New Delhi, India. 3-(4,5-dimethyl-2-yl)-2,5-dip henyltetrazolium bromide (MTT) and Phosphate-buffered saline (PBS) were procured from Himedia Laboratory Pvt. Ltd, Mumbai, India. Phosphate-buffered saline (PBS) was procured from Calbiochem, Merck India Pvt. Ltd, Mumbai, India. Propidium iodide, N-acetyl L-tryptophan, radioimmune precipitation assay (RIPA) lysis buffer, Bradford reagent, paraffin, xylene, sodium citrate, Tween 20, and DAB were purchased from Sigma-Aldrich, St Louis, MO. All Elisa kits i.e. Lgr-5, Bmi-1, Msi-1, Dclk-1, G-CSF, IL-6, NFkB and IL-12 were bought from Bioassay Technology Laboratory (Shanghai, China). G- CSF, IL-6, NFkB and IL-12 Elisa kits were procured from Biostring Inc, USA. SP Elisa kits were procured from Finetest, Wuhan, China. All other chemicals used were of analytical grade and standard make.

Methods

A comparative molecular docking analysis to determine L-NAT and capsaicin binding with TRPV1 receptor

Molecular docking analysis of L-NAT, and capsaicin with TRPV1 [(PDB; Sequence: 7L2H-1 *Rattus norvegicus* (10116)] receptor was performed using AutoDock vina (CB-dock2) tools. The molecular interactions, animo acid residues of TRPV1 receptor involving in the binding with L-NAT and capsaicin was identified and compared.

Estimation of substance P expressions in the serum and intestinal tissue of L-NAT, capsaicin treated and gamma radiation exposed mice

To determine the effect of gamma radiation on substance P expression and its modulation by L-NAT pretreatment, mice were divided into following seven groups and each experimental group having six animals:

1. Control animals: animals were injected (im) with vehicle control, (n = 6).
2. Mice injected with capsaicin (16 mg/kg, iv), (n = 6).
3. Mice treated with L-NAT (150 mg/kg, b.wt im) 90 minutes before capsaicin treatment (16 mg/kg, iv) treatment, (n = 6).
4. Mice injected with capsaicin (16 mg/kg, iv) 30 minutes before L-NAT administration (150 mg/kg, b.wt im), (n = 6).
5. Mice injected with L-NAT (150 mg/kg, b.wt. im), (n = 6).
6. Mice exposed with gamma radiation (9.0 Gy; whole body) (n = 6).
7. Mice injected with L-NAT (150 mg/kg, b.wt. IM) 2h before gamma radiation exposure (9.0 Gy; whole body).

Followed by treatments, mice were incubated for 2h and thereafter animals were sacrificed and blood and jejunum section of small intestine was collected. To estimate the substance P level in the serum and small intestine, tissues were processed to extract the total soluble proteins and Elisa assay was performed as per instruction provided by the Elisa kit manufacturer. An equal amount of protein was poured into the Elisa plate wells and plates incubated at 37 °C for 90 minutes. Thereafter, the plates were washed with a washing buffer. 100 µl of biotin-labeled antibodies were added into the wells and further allowed to incubate for 60 minutes at 37 °C. Afterwards, 100 µl of streptavidin-biotin complex (SABC)

was mixed to each well and left for 30 minutes of incubation at 37 °C. In each well, 90 µl of 3,3′,5,5′-Tetramethylbenzidine (TMB) substrate was mixed and again kept for 30 minutes of incubation at 37 °C. Then, 50 µl of stop solution was mixed to stop the reaction. The optical density of the color complex was measured at a wavelength of 450 nm using a spectrofluorometer (Synergy, BIO-TEK Powerwave XS2, USA)

In vivo radioprotective efficacy determination

Irradiation of the mice

C57Bl/6 mice (Male/Female) were irradiated with gamma radiation using a Bhabhatron-II Telecobalt irradiator (Bhabha Atomic Research Center, Mumbai, India) having ^{60}Co source of gamma radiation with dose rate: 1.4-1.36 Gy/min, and field area 35x35cm with 80SSD. The Bhabhatron-II Telecobalt irradiator's radiation beam was calibrated by medical physicist and radiation safety officers of the institute following IAEA's TRS-398 protocol using calibrated Farmer type, 0.6 cc volume ionization chamber in water phantom. The dose rate measured at 80SSD was 1.4-1.36 Gy/minutes within the time duration (months periods) of mice experiments. Animals were placed in prone position individually and irradiated using perforated plastic containers. The prescribed dose of radiation was calculated at the mid plane of the torso region of the mice by qualified medical physicist of the institute. No tissue heterogeneity corrections were applied for specific organs. During all the animals' experiments, Institutional Animal Ethical Committee (IAEC) instructions were strictly followed. All animal experiments were undertaken with due approval from IAEC.

Preparation of L-NAT doses and mode of administration

L-NAT (1.0 mg) was freshly dissolved in 900 µl of distilled water and shaken well for 10 minutes using cyclomixture. 90 µl of 10 M sodium hydroxide was added and shaken for 1 minute at room temperature. The final solution was made up to 1500 µl using distilled water. The pH of the final solution was fixed as 7.0 with the help of 0.1 N HCl. Dose volume of L-NAT injection (IM) was calculated using the following formula:

$$\text{Dose volume} = \text{body weight of the animal}(g)\,x\,\text{Dose} / 1000x\,\text{concentration of test molecule}(mg/ml)$$

Evaluation of acute toxicity and maximum tolerable dose (MTD) of L-NAT in mice

To determine the acute toxicity and maximum tolerable dose (MTD) of N-acetyl-L-tryptophan, toxicity (GLP) studies were carried out at the GLP facility at Sri Ramachandran University (SRU), Chennai. The study was conducted according to schedule Y of Drugs and Cosmetic act, Ministry of Health and Family welfare, Government of India, 2005 and OECD series on Principles of Good Laboratory Practice and Compliance Monitoring, number 1, ENV/MC/CHEM (98) 17. In brief, animals were divided into four groups and each group having 5 mice. Animals were administered with escalating doses of L-NAT as:

Group 1: Mice administered with 250 mg/Kg, b.wt (n = 5)
Group 2: Mice administered with 500 mg/Kg, b.wt (n = 5)
Group 3: Mice administered with 1000 mg/Kg, b.wt (n = 5)
Group 4: Mice administered with 1500mg/Kg, b.wt (n = 5)

Followed by all treatments, animal's body weight was recorded on day 0 (before dosing), day 7 and day 14. Mortality and morbidity were recorded twice daily till necropsy. Clinical signs, if any, were recorded approximately at 30 min, 1, 2 and 4h on day 0 (after L-NAT administration) and thereafter, once daily till necropsy. All surviving animals were euthanized for gross pathology on day 14. Acute toxicity of L-NAT was observed in terms of percent survival, changes in behavior, morbidity and mortality. The maximum concentration of L-NAT at which nominal toxic manifestations initiated was considered as maximum tolerance dose (MTD).

L-NAT radioprotective efficacy determination in mice

To evaluate the radioprotective efficacy of **L-NAT**, animals were divided into following four experimental groups, each group having six animals:

1. Control animals (n = 6): Mice injected (IM) with vehicle control
2. L-NAT treated animals (n = 6): Mice injected with different doses of L-NAT (100-200 mg/Kg, b.wt. IM)
3. Gamma radiation exposed animals (n = 6): Mice irradiated with gamma radiation (9 Gy; whole body)
4. L-NAT treated and irradiated animals (n = 6): Mice injected with L-NAT (100-200 mg/Kg, b.wt. IM) 2h before irradiation (9 Gy; whole body).

All animals were observed for 30 days for any signs of radiation sickness, behavioral toxicity, morbidity and mortality (Malhotra et al. 2019). Data was presented as the percentage (%) survival of the irradiated group of mice that were injected with L-NAT compared to the irradiated group of mice that not preinjected with L-NAT The optimum dose at which maximum whole-body survival achieved was used for further investigations.

Determination of optimum time window to achieve maximum L-NAT mediated radioprotection in mice

To optimize the time window for L-NAT mediated radioprotection, male C57bl/6 mice were divided into following six groups:

1. Mice injected with vehicle control, (n = 6)
2. Mice exposed with gamma radiation (9.0 Gy), (n = 6)
3. Mice injected with L-NAT (150 mg/Kg, b.wt.im), (n = 6)

4. Mice treated with L-NAT (150mg/Kg, b.wt) 30 minutes before gamma radiation exposure (9.0 Gy), (n = 6)
5. Mice treated with L-NAT (150mg/Kg, b.wt) 1h before gamma radiation exposure (9.0 Gy), (n = 6)
6. Mice treated with L-NAT (150mg/Kg, b.wt) 2h before gamma radiation exposure (9.0 Gy), (n = 6)
7. Mice treated with L-NAT (150mg/Kg, b.wt) 3h before gamma radiation exposure (9.0 Gy), (n = 6)

All animals were monitored up to 30 days for any appearance of radiation sickness, behavioral toxicity, morbidity and mortality (Malhotra et al. 2019). Data was presented as the percentage (%) survival of the irradiated group of mice that were preinjected with L-NAT. The optimum time window at which maximum whole-body survival achieved was used for further experimentation.

L-NAT dose reduction factor (DRF) determination in mice

The dose reduction factor for L-NAT was calculated at efficacy dose (150 mg/Kg, b.wt.im) using radiation dose LD_{50} as the baseline. In brief, male C57bl/6 mice were divided into following experimental groups:

1. Mice irradiated with 5 Gy dose of gamma radiation (n = 6)
2. Mice irradiated with 6 Gy dose of gamma radiation (n = 6)
3. Mice irradiated with 7 Gy dose of gamma radiation (n = 6)
4. Mice irradiated with 8 Gy dose of gamma radiation (n = 6)
5. Mice irradiated with 9 Gy dose of gamma radiation (n = 6)
6. Mice irradiated with 5 Gy gamma radiation dose, 2h after L-NAT (150mg/Kg, b.wt.im) treatment (n = 6)
7. Mice irradiated with 6 Gy gamma radiation dose, 2h after L-NAT (150mg/Kg, b.wt.im) treatment (n = 6)
8. Mice irradiated with 7 Gy gamma radiation dose, 2h after L-NAT (150mg/Kg, b.wt.im) treatment (n = 6)
9. Mice irradiated with 8 Gy gamma radiation dose, 2h after L-NAT (150mg/Kg, b.wt.im) treatment (n = 6)
10. Mice irradiated with 9 Gy gamma radiation dose, 2h after L-NAT (150mg/Kg, b.wt.im) treatment (n = 6)
11. Mice irradiated with 10 Gy gamma radiation dose, 2h after L-NAT (150mg/Kg, b.wt.im) treatment (n = 6)
12. Mice irradiated with 12 Gy gamma radiation dose, 2h after L-NAT (150mg/Kg, b.wt.im) treatment (n = 6)

Followed by completion of radiation and L-NAT treatments, mice were transferred to institutional animal facility and kept under observations. The mortality occurs in different experimental groups were reported. The whole-body survival (%) of irradiated mice that pretreated with L-NAT was compared with the survival (%) of radiated mice that not pretreated with L-NAT (Abdi et al. 2018). DRF for L-NAT was calculated as the ratio of mice survival (%) achieved at LD_{50} radiation dose without L-NAT treatment and 50% survival of the mice achieved upon L-NAT pretreatment (150 mg/Kg, b.wt im) to irradiated mice at 30 days survival (%) timescale.

Histological analysis of jejunum section of small intestine of irradiated and L-NAT pretreated mice

Following euthanasia, the jejunum section of the small intestine of irradiated and L-NAT pretreated mice was collected at different time intervals (day 3, 7 and 14). Fat and connective tissues attached with jejunum section were carefully scrapped out. Intestinal tissue was fixed in buffered paraformaldehyde at room temperature for 24h. Subsequently, the tissue specimens underwent dehydration using a series of graded ethanol and were then embedded in paraffin blocks. For H&E staining, 5 µm thick TS sections were prepared. Quantitative analysis of the histology of jejunum sections was carried out manually under a microscope (Azmoonfar et al. 2023). Digital images of the stained sections were captured and subjected to quantitative analysis using NIS element software integrated with an automated microscope (Nikon Ti series, Japan). At least 5 slides were prepared from each experimental group and 4 tissue sections were analyzed per slides. However, in radiation control group, where animals' death occurs within 14 days, 2-3 slides were prepared. Therefore, total 20 tissue sections per parameter were analyzed per experimental groups except radiation control group, where only 8-12 tissues sections per parameter were studied at one time point.

Expression analysis of intestinal stem cell markers

Intestinal stem cell markers (i.e. Lgr-5, Bmi-1, Msi-1, Dclk-1) expressions were estimated using Elisa assay (Yan et al. 2012). Animals were divided into four experimental groups as mentioned above. After completion of the desired incubation time followed by radiation and L-NAT treatments, expression of intestinal stem cell markers was analyzed. In brief, protein (100 µl) extracted from jejunum sections was added into elisa plats wells and incubated for 90 minutes at 37 °C. Thereafter, the elisa plate was washed with washing buffer and biotin labeled detection antibody (100 µl) added and again incubated for 60 minutes at 37 °C. Furthermore, HRP-Streptavidin Conjugate (SABC; 100 µl) was added to each well and incubated for 30 minutes at 37 °C. Then, 90 µl of 3,3′,5,5′-Tetramethylbenzidine (TMB) substrate mixed in each well and, incubated for 30 minutes. A stop solution (50 µl) was added to wells to stop the reaction. The absorbance was measured at 450 nm by a spectrofluorometer (Synergy, BIO-TEK Powerwave XS2, USA). Quantitative estimation of expression of individual markers was carried out by extrapolation in terms of pg/mg of protein obtained from a standard curve prepared in parallel using a standard of individual markers supplied with the individual kits.

Determination of hematopoietic system radioprotection offered by L-NAT in irradiated mice

Followed by euthanasia, femur bone was collected from irradiated and L-NAT pretreated mice at days 3, 7 and 14 post treatment periods. Muscles and connective tissues attached to the bones were carefully scrapped out. Bone tissue was fixed in buffered para-formaldehyde at room temperature for 24h. Subsequently, the tissue specimens underwent dehydration using a series of graded ethanol and were then embedded in paraffin blocks. For H&E staining, 5 µm thick LS sections were prepared. Quantitative analysis of histological sections of bone marrow was carried out manually under microscope (Travlos 2006; Meza-León et al. 2021). Digital images of the stained sections were captured and subjected to quantitative analysis using NIS element software integrated with an automated microscope (Nikon Ti series, Japan).

Evaluation of male reproductive system radioprotective activity of L-NAT

Followed by euthanasia, right and left testicles were collected from irradiated (8 Gy) and L-NAT pretreated mice at day 7, 14, 21, 28 and 35 post treatment periods. Muscles and associated connective tissues attached to the testicles were carefully removed. Both testicles were fixed in buffered paraformaldehyde at room temperature for 24h. Subsequently, the tissue specimens underwent dehydration using a series of graded ethanol and were then embedded in paraffin blocks. For H&E staining, 5 µm thick TS sections were prepared. Quantitative analysis of histological sections of testicles was carried out manually under a microscope (Kaur et al. 2023). Digital images of the stained sections were captured and subjected to quantitative analysis using NIS element software integrated with an automated microscope (Nikon Ti series, Japan).

L-NAT radioprotective efficacy determination in NHPs (Macaca mulata)

Irradiation of NHPs

To evaluate the radioprotective efficacy of L-NAT, NHPs (*Macaca Mulata*; male and female) were used. Animals were irradiated with gamma radiation using a Bhabhatron-II Telecobalt irradiator (Bhabha Atomic Research Center, Mumbai, India) having dose rate: 0.318 Gy/min, and field area 63x63cm with 120 SSD). Animals were irradiated individually under anesthesia. During NHP studies, the Institutional ethical committee and CPSCEA safety guidelines were strictly followed. All animal experiments were undertaken with IAEC and CPSCEA approvals (No. 25/17/2019-CPCSEA).

A dosimetry exercise was performed before experimentation to ensure desired dose delivery to the individual Macaque. In brief, a cobalt^{60} Teletherapy (Model: Bhabhatron-II, Panacea Medial Technologies Pvt. Ltd. India) machine was used to whole-body irradiation of NHP in prone position, single animal at a time at source to surface distance (SSD) of 120 cm to cover the full length of the NHP. The teletherapy beam was calibrated following IAEA's TRS-398 protocol using a calibrated Farmer type 0.6 cc volume ionization chamber in a water phantom. The dose rate measured at the extended SSD was 0.318 Gy/min. The prescribed dose was 6.5 Gy at the mid-plane of the torso region of the individual NHP. The delivered dose was calculated by the institute's medical physicist, without applying tissue specific heterogeneity correction.

L-NAT mice to NHP dose conversion calculation

Rhesus Macaque equivalent dose (MED) of L-NAT was extrapolated using the following calculation (Sharma and McNeill 2009; Nair and Jacob 2016) based on body surface area (adapted from FDA guidelines):

Rhesus Macaque equivalent dose (MED) = Dose in mice (mg/kg) x dose conversion factor of mice (mg/Kg, b.wt.) Km (Mice)/Dose conversion factor of Rhesus Macaque (mg/Kg, b.wt.) Km (Rhesus Macaque)

L-NAT radioprotective activity evaluation in non-human primate model

To evaluate the radioprotective activity of **L-NAT**, *Macaca mulata* aged 8-10 years, weight 7-10 kg male and female macaque were used for experimentation. The overall health of individual animals was monitored in terms of their hematology profile, biochemistry parameters, liver function tests and kidney function tests before experiments initiation. Approval from Institutional Animal Ethical Committee (IAEC) and CPSCEA Ministry of Environment, Govt. of India was granted (No. 25/17/2019-CPCSEA; dated 25/09/2019) to conduct the study with duly safety guidelines in placed.

In brief, animals were divided into following four experimental groups:

1. Control animals (n = 4): Macaque injected (im) with vehicle control, (n = 4).
2. L-NAT treated animals (n = 4): Macaque injected with L-NAT (37.5 mg/Kg, b.wt. im), (n = 4).
3. Gamma radiation exposed animals (n = 4): Macaque irradiated with gamma radiation (6.5 Gy; whole body) (n = 4).
4. L-NAT treated and then irradiated animals (n = 4): Macaque injected with L-NAT (37.5 mg/Kg, b.wt. im) 2h before irradiation (6.5 Gy; whole body), (n = 4).

Note: out of 4 animals used for each experimental group, male:female ratio was 50:50

Followed by all treatments, animals were kept at Non-Human Primate Facility, National Institute of Immunology, Delhi, for subsequent monitoring of mortality, morbidity, facial inflammation, behaviors changes, food intake patterns, hematology profile, liver function tests, kidney function tests, blood biochemistry, and histopathological analysis of

the dead animals (Burdelya et al. 2008). No supportive care was provided to any experimental group of NHPs during entire duration of experiments.

Note: NHP survival study experiment was performed once only.

Hematology and blood biochemistry analysis of irradiated and L-NAT pretreated NHPs

Followed by L-NAT and radiation treatments as mentioned above, all animals were kept under observations. To determine the effect of gamma radiation on hematological, liver function test, and kidney function tests parameters of irradiated animals with or without L-NAT pretreatment, blood samples were collected at different time intervals, i.e. 2, 10, 14, 20. 30 day and 7th month and analyzed. The blood profiles of individual experimental animals were also analyzed before initiation of L-NAT and gamma radiation treatments (0 h) as control for follow-up comparison (Burdelya et al. 2008).

Evaluation of G-CSF, IL-6, IL-12 and NFkB cytokines expression in the serum of NHP upon L-NAT escalating dose administration

To determine the efficacy biomarker for L-NAT, cytokines i.e. G-CSF, IL-6, NFkB and IL-12 expression analysis was performed using Elisa assay. In brief, following experimental groups were formed:

1. Control: animals administered with vehicle control (n = 4; male)
2. Animals administered with 1x dose (37.5 mg/kg b.wt. im) of L-NAT (n = 4; male)
3. Animals administered with 2x dose (75 mg/kg b.wt. im) of L-NAT (n = 4; male)
4. Animals administered with 3x dose (112.5 mg/kg b.wt.im) of L-NAT (n = 4; male)

Blood (3 ml) was collected from individual animal after 2h of L-NAT administration. Serum was separated from the blood samples using centrifugation at 2000 rpm for 10 minutes at room temperature using swing bucket rotor. Elisa assay was performed to analyze G-CSF, IL-6, NFkB and IL-12 cytokine expressions using respective Elisa kits (Biostring Inc, USA).

In brief, an equal amount (50 µl) of serum samples was added to the per-coated wells of the Elisa plate and kept at 37 °C for 90 minutes. After that, the plate was rinsed with a washing buffer. 100 µl of biotin-labeled antibody was added into the wells and allowed to incubate for 60 minutes at 37 °C. Afterwards, 100 µl of SABC (streptavidin-biotin complex) was added to each well and left for 30 minutes of incubation at 37 °C. In each well, 90 µl of TMB substrate was mixed and again left for 30 minutes of incubation at 37 °C. Then, 50 µl of stop solution was added to stop the reaction. The optical density of the color complex was measured at a wavelength of 450 nm using a spectrometer (Synergy, BIO-TEK Powerwave XS2, USA).

Statistical analysis

All experiments except NHPs radioprotection studies were repeated at least three times and data were expressed as mean and standard deviation. NHP studies were conducted only once. The variations between the control, radiation-treated, and L-NAT pretreated plus irradiated groups of mice were estimated using one-way ANOVA (one-way analysis of variance) with Tukey's test using Prism 8.0.1 (Graph Pad Software, San Diego, CA, USA. The significance of variance (p-value) within treatment groups was considered <0.05 unless specified otherwise.

Results

L-NAT interacts with TRPV1 receptor

Molecular docking analysis demonstrated an almost equally comparable binding of L-NAT (binding energy of −8.0; binding pocket C1) with TRPV1 receptor as TRPV1 agonist capsaicin (binding energy of −8.2; binding pocket C4). Interestingly, the best fit pockets (binding sites), binding cavity volume and binding sites coordinates of TRPV1 receptor for L-NAT and capsaicin binding (Figure 1a, b) were also found exactly similar. Besides that, 25 amino acids of TRPV1 receptor (Figure 1b) was identified in the best fit binding pocket C1 that commonly interact with both ligands i.e. L-NAT and capsaicin suggesting close competitiveness among them toward TRPV1 interaction.

Substance P expression modulation by radiation and L-NAT and TRPV1 agonist capsaicin treatments in mice

Significant ($p < .0299$) induction of substance P level was observed in the intestine of mice upon capsaicin treatment. Though, moderate inhibition in substance P level was observed in the serum ($p = .05$). However, significant inhibition of substance P expression was observedin the intestine ($p < .0162$) of mice that were treated with L-NAT as compared to untreated control (Figure 1c,d). More interestingly, significant) inhibition in substance P level was evident in the serum ($p < .0008$) and intestine ($p < .0009$) of irradiated (9 Gy) mice that preinjected with L-NAT compared to the irradiated (9 Gy) mice that were not preinjected with L-NAT. Therefore, present findings were clearly demonstrated that irradiation enhanced substance P expression in the serum and intestine of the irradiated mice, whereas, L-NAT pretreatment effectively inhibit substance P expression predominantly in both the tissues.

Evaluation of in vivo radioprotective activity of L-NAT using mice model

Single dose acute toxicity profiling of L-NAT

The single dose acute toxicity studies were performed as per Drugs and Cosmetic rules, Ministry of Health and Family Welfare, Government of India, 2005 and OECD series on principles of good laboratory practice and compliance

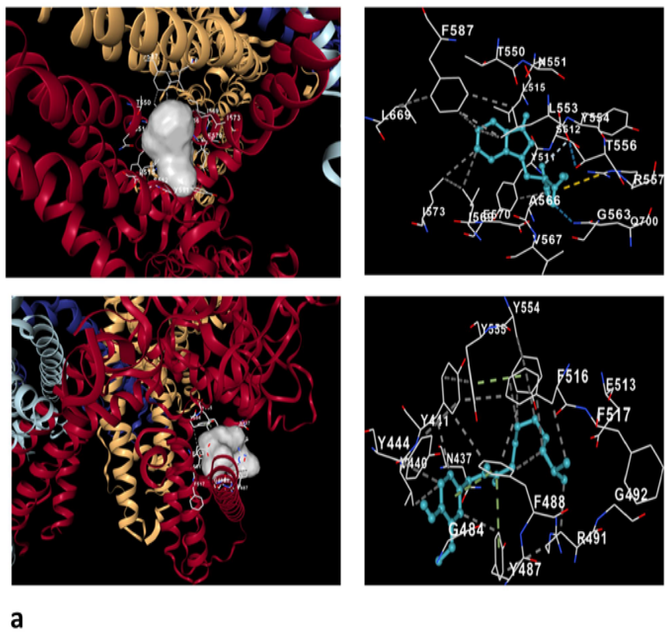

NAT-TRPV1 docking

CurPocket ID	Vina score	Cavity volume (Å3)	Center (x, y, z)	Docking size (x, y, z)
C1	-8.0	6825	101, 140, 122	31, 32, 33
C2	-8.0	6677	123, 99, 126	31, 35, 35
C3	-7.9	5386	140, 163, 128	31, 33, 34
C4	-7.9	5280	162, 122, 123	30, 31, 33
C5	-7.1	915	122, 88, 157	19, 19, 31

Cap-TRPV1 docking

CurPocket ID	Vina score	Cavity volume (Å3)	Center (x, y, z)	Docking size (x, y, z)
C4	-8.2	5280	162, 122, 123	30, 31, 33
C1	-8.1	6825	101, 140, 122	31, 32, 33
C3	-7.9	5386	140, 163, 128	31, 33, 34
C2	-7.8	6677	123, 99, 126	31, 35, 35
C5	-6.4	915	122, 88, 157	21, 21, 31

TRPV1 receptor 's common amino acids residues involved in interaction with L-NAT and Capsaicin in binding pocket C1
VAL508, ASP509, SER510, TYR511, SER512, GLU513, LEU515, PHE516, THR550, ASN551, LEU553, TYR554, TYR555, THR556, ARG557, GLY563, ALA566, VAL567, ILE569, GLU570, LYS571, ILE696, LEU699, GLN700, ILE703

b

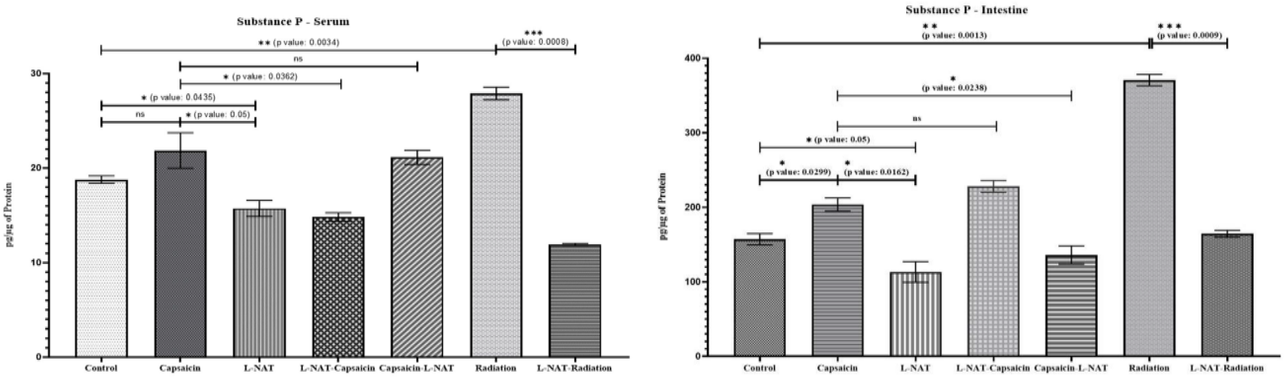

c d

Figure 1. L-NAT mediated TRPV1 receptor blocking and subsequent substance P expression inhibition analysis. L-NAT and capsaicin (a) binding with TRPV1 receptor was analyzed using autodock vina tools. The TRPV1 receptor's amino acid residues participating in the binding with L-NAT and capsaicin, binding energy, binding sites coordinates, binding cavity volume and docking size parameters were recorded and compared (b). Substance P expression in the serum (c) and small intestine (d) of mice upon L-NAT, capsaicin (TRPV1 agonist), gamma radiation and their combined treatment was analyzed. Data were represented as mean ± SD of three independent experiments. Significance of variance was considered as p value <0.05: **Serum:** ns; control Vs capsaicin treatment ($p > .05$); *; control Vs L-NAT treatment ($p < .0435$); *; capsaicin treatment Vs L-NAT treatment ($p < .0362$); **; control Vs radiation treatment ($p < .0034$); ***; radiation treatment Vs L-NAT+radiation treatment ($p \leq 0.0008$), **intestine:** *; control Vs capsaicin treatment ($p < .0299$); control Vs L-NAT treatment ($p < .05$); *; capsaicin treatment Vs L-NAT treatment ($p < .0162$); **; control Vs radiation treatment ($p < .0013$); ***; radiation treatment Vs L-NAT+radiation treatment ($p \leq 0.0009$). ns: non significant.

monitoring, No. ENV/MC/CHEM (98)17 (study No. 1155/2018). Animals injected (IM) with four graded doses (250, 500, 1000, 1500 mg/Kg, b.wt; im) did not show any signs of toxicity. No mortality and morbidity were observed throughout experimental period, i.e. days 14. No gross lesions were observed in any of the organs of the animals during the histopathological analysis done. All groups of animals treated with L-NAT showed an increase in body weight on day 7 compared to their day 0 body weight. However, a decrease in total body weight was observed on day 14 in group 3 (5/5) and group 4 (2/5) as compared to their body weight on day 7. Though, there was no mortality observed in any groups of animals. However, based on clinical signs, mortality/morbidity and gross pathology, the LD50 dose of L-NAT was considered to be 1500 mg/Kg, b.wt., under experimental conditions.

Data on days 14 repeat dose toxicity (GLP) in non-rodent model (New Zealand white rabbits), genotoxicity (mutagenesis, chromosomal abrasion, micronuclei), and male reproductive system toxicity has been generated and archived with us (Data not shown). No-observed adverse effect level (NOEL) of L-NAT was observed in rodent and non-rodent models.

In vivo L-NAT radioprotective activity determination using mice model

To evaluate the radioprotective activity of L-NAT against a lethal dose of gamma radiation, the animals were injected with different doses (100, 125, 150, 200 mg/Kg, b.wt. im) of L-NAT 2h before whole body irradiation and 30 days survival (%) of all animals observed. Observations of the study demonstrated a

maximum enhancement (>83%) in the survival (%) of the irradiated (9.0 Gy) mice that were pretreated (-2h) with L-NAT (150 mg/Kg, b.wt., im) compared to the irradiated (9.0 Gy) mice that does not preinjected with L-NAT (Figure 2). However, further increase in L-NAT concentration (200 mg/Kg, b.wt.) led to a significant decrease (p = .017) in the survival (33.3%) of irradiated mice as compared to the mice treated with 150 mg/Kg, b.wt. of L-NAT (Figure 2). Therefore, the present study demonstrated significant radioprotective activity of L-NAT at 150 mg/Kg, b.wt (im) in irradiated mice.

Determination of prophylactic time window of L-NAT

To optimize the time window for L-NAT radioprotective activity against gamma radiation induced lethality, animals were injected with L-NAT (150 mg/Kg, b.wt.im) before 30 minutes, 1h, 1.5h, 2h and 3h before irradiation (9.0 Gy) and whole body 30 days survival (%) of irradiated animals were monitored. Maximum survival (~83%) was observed at 2h before L-NAT treatment to irradiated mice. However, a significant ($p < .05$) reduction in the survival (%) of the irradiated mice was observed upon deviation from the 2h time window between L-NAT injection (im) and radiation exposure (Figure 3). Interestingly, no survival was observed with the mice treated with L-NAT 30 minutes before irradiation. However, a significant reduction in percent (%) survival was observed with irradiated mice that preinjected with L-NAT before1h (16.6%), 1.5h (50%), and 3h (33.3%) respectively (Figure 3).

Dose reduction factor (DRF) estimation

To determine the dose reduction/modification factor (DRF/DMF) for L-NAT, mice were irradiated with or without L-NAT (150 mg/Kg, b.wt.) pretreatment and 30 days whole body survival percentage (%) was estimated. The LD_{50} radiation dose of C57BL/6 male/female mice was estimated to be 7.0 Gy as extrapolated using a logarithmic scale, while it was found to be 7.5 Gy without logarithmic scale calculation (Figure 4). In contrast, as the results of L-NAT pretreatment (150 mg/Kg, b.wt.), 50% survival of the irradiated mice was achieved at 10 Gy radiation dose (with logarithmic and non-logarithmic plot; Figure 4). Therefore, the DRF/DMF value estimated on the basis of 50% survival of irradiated mice with or without L-NAT pretreatment to be 1.42 with Logarithmic scale calculation and 1.33 with non-Logarithmic scale calculation.

L-NAT mediated protection to gastrointestinal system of irradiated mice

The L-NAT radioprotective formulation was developed and evaluated for its systemic radioprotection efficacy in mice model. Radioprotection to the gastrointestinal system against lethal dose of whole-body gamma radiation was studied using qualitative and quantitative histological analysis. Significant cellular damage in terms of villi length reduction, villi width enhancement, crypt cell degeneration, crypt mitotic cells and goblet stem cells reduction was observed in the jejunum of irradiated mice that was not pretreated with L-NAT compared to controls (Figure 5a,b,c,d). However, pretreatment of the irradiated mice with L-NAT was found to be a contributing factor to protect the mice GI system against radiation-induced damage. In brief, being the second most radiosensitive system, radioprotection of the GI system by L-NAT pretreatment may be a major factor to ensure survival of the irradiated mice.

Quantitative histological analysis of small intestine (jejunum) of irradiated and L-NAT pretreated mice

Quantitative analysis of the small intestine (jejunum) was performed using an automated motorized microscope equipped

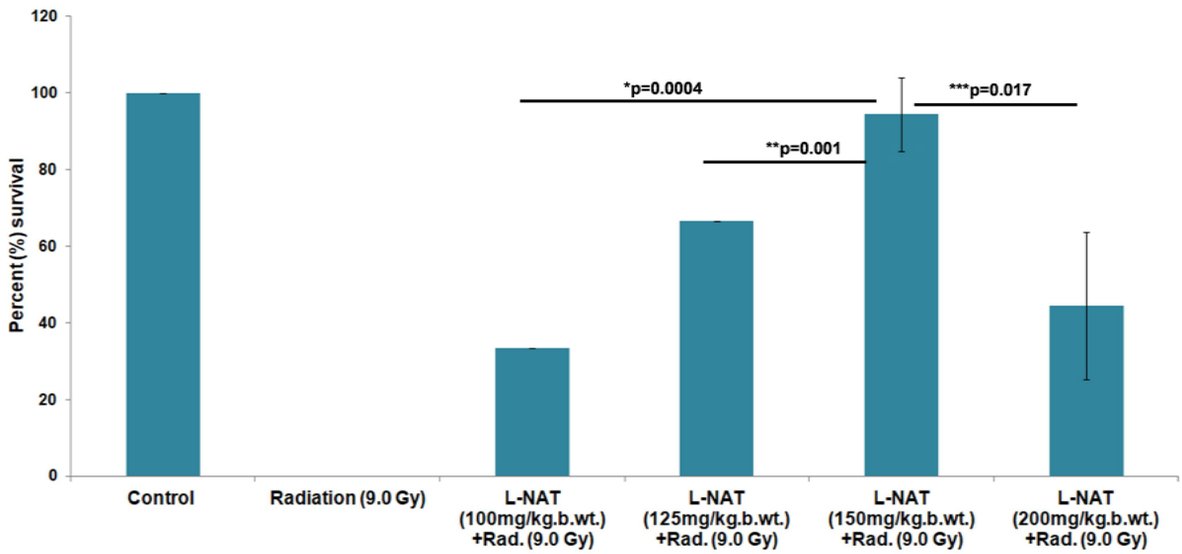

Figure 2. Radioprotective activity of L-NAT in C57BL/6 mice. Different concentrations (100-200 mg/Kg, b.wt.im) of L-NAT were injected (-2h) to the irradiated groups ($n = 6$) of C57BL/6 mice and 30 days survival (%) was monitored and compared with the survival (%) of the irradiated (9.0 Gy) group of mice that not pretreated with L-NAT. Data were represented as mean ± SD of three independent experiments. The significance of variance was considered as p value <0.05. *,L-NAT (100 mg/kg) + radiation (9.0 Gy) Vs L-NAT (150 mg/kg)+ radiation (9.0 Gy), $p = .0004$; **, L-NAT (125 mg/kg) + radiation (9.0 Gy) Vs L-NAT (150 mg/kg)+ radiation (9.0 Gy), $p = .001$; ***, L-NAT (150 mg/kg) + radiation (9.0 Gy) Vs L-NAT (200 mg/kg)+ radiation (9.0 Gy), $p = .017$.

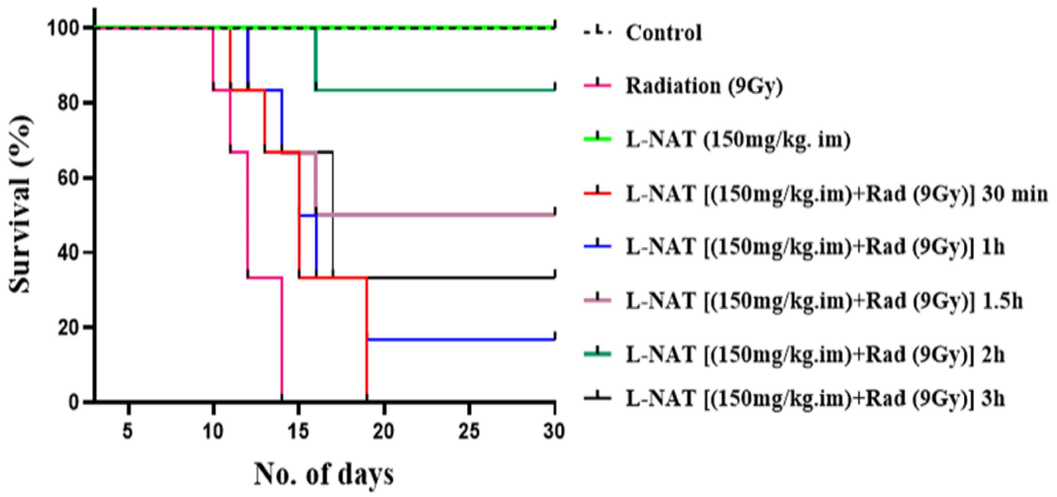

Figure 3. Determination of optimum time window to achieve maximum radioprotection by L-NAT mice. Each experimental group has six mice (n = 6). Mice were injected with L-NAT (150 mg/Kg, b.wt.im) 30 minutes, 1h, 1.5h, 2h, and 3h before irradiation (9.0 Gy) and 30 days whole body survival (%) was estimated.

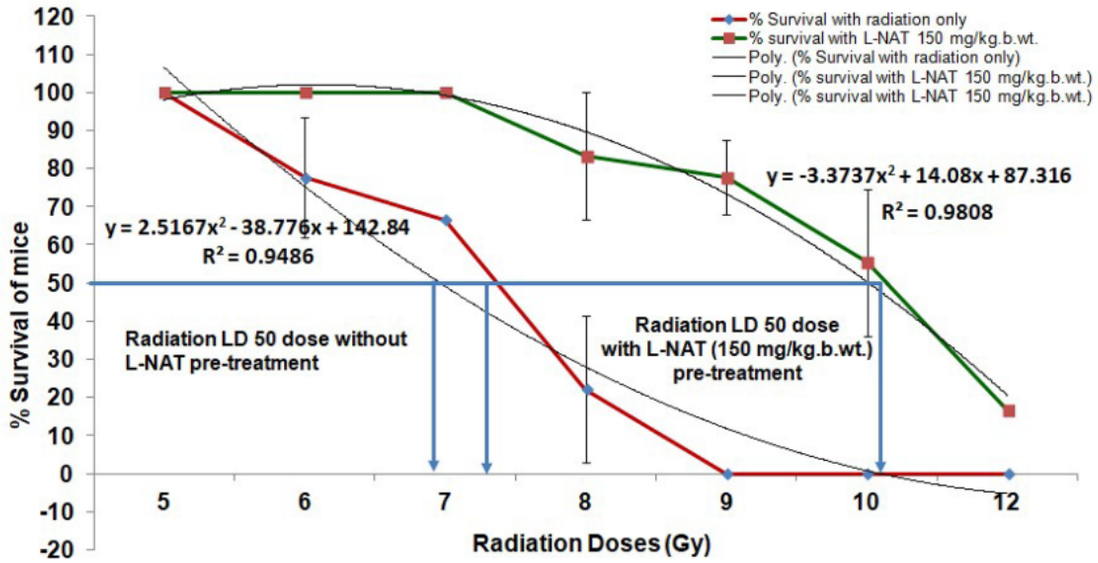

Figure 4. **L-** NAT dose reduction factor determination using C57BL/6 mice. Dose reduction factor for L-NAT radioprotective efficacy was determined by calculating the ratio of survival % at radiation dose LD_{50} without L-NAT pretreatment and with L-NAT (150 mg/kg) pretreatment. The DRF value for L-NAT was calculated to be 1.42 with logarithmic scale and 1.33 without using the logarithmic scale of calculation. Data were represented as mean ± SD of three independent experiments.

with NIS element analysis software. Significant reduction in the length of villi was observed with irradiated mice at all tested time points (days 3-14). However, maximum reduction in the villi length (~80%; p = .0017), epithelial enterocytes/villus (~70%; p = .001) and number of goblet cells/villus (~86%; p = .00048) was noticed at day 14 in irradiated mice (Figure 5e,g,h) compared to untreated control group of mice. Whereas, a significant increase in the villi width was observed with irradiated mice that were not pretreated with L-NAT compared to untreated control mice (p = .0085) as well as irradiated mice that were pretreated with L-NAT (p = .0075; Figure 5f), suggested cellular edema and inflammation in damaged villi. Therefore, as the results of L-NAT pretreatment, villi length, epithelial enterocytes/villus and number of goblet cells/villus was found significantly protected in irradiated mice compared to the irradiated mice that were not pretreated with L-NAT (Figure 5e–h).

Quantitative analysis of intestinal crypt cells

Significant reduction in the number of crypts/villus section, number of cells/crypt, number of mitotic cells, and number of goblet cells/crypt was observed with irradiated mice that were not pretreated with L-NAT at all tested time points (3, 7 and 14 days). However, the maximum reduction in the number of crypts/villus section (p = .028), number of cells/crypt p = 0.006), number of mitotic cells/crypt (p = .0029), number of goblet cells/crypt (p = .007) was noticed at day 14 in irradiated mice (Figure 6a,b,c,d) compared to the untreated control group of mice. As the results of L-NAT pretreatment to the irradiated mice, the number of crypts/villus section (p = .042), number of cells/crypt (p = .0001), number of mitotic cells/crypt (p = .0008), number of goblet cells/crypt (p = .0002) was found significantly protected compared to the irradiated mice that were not pretreated with L-NAT (Figure 6e–h). Interestingly, a significant

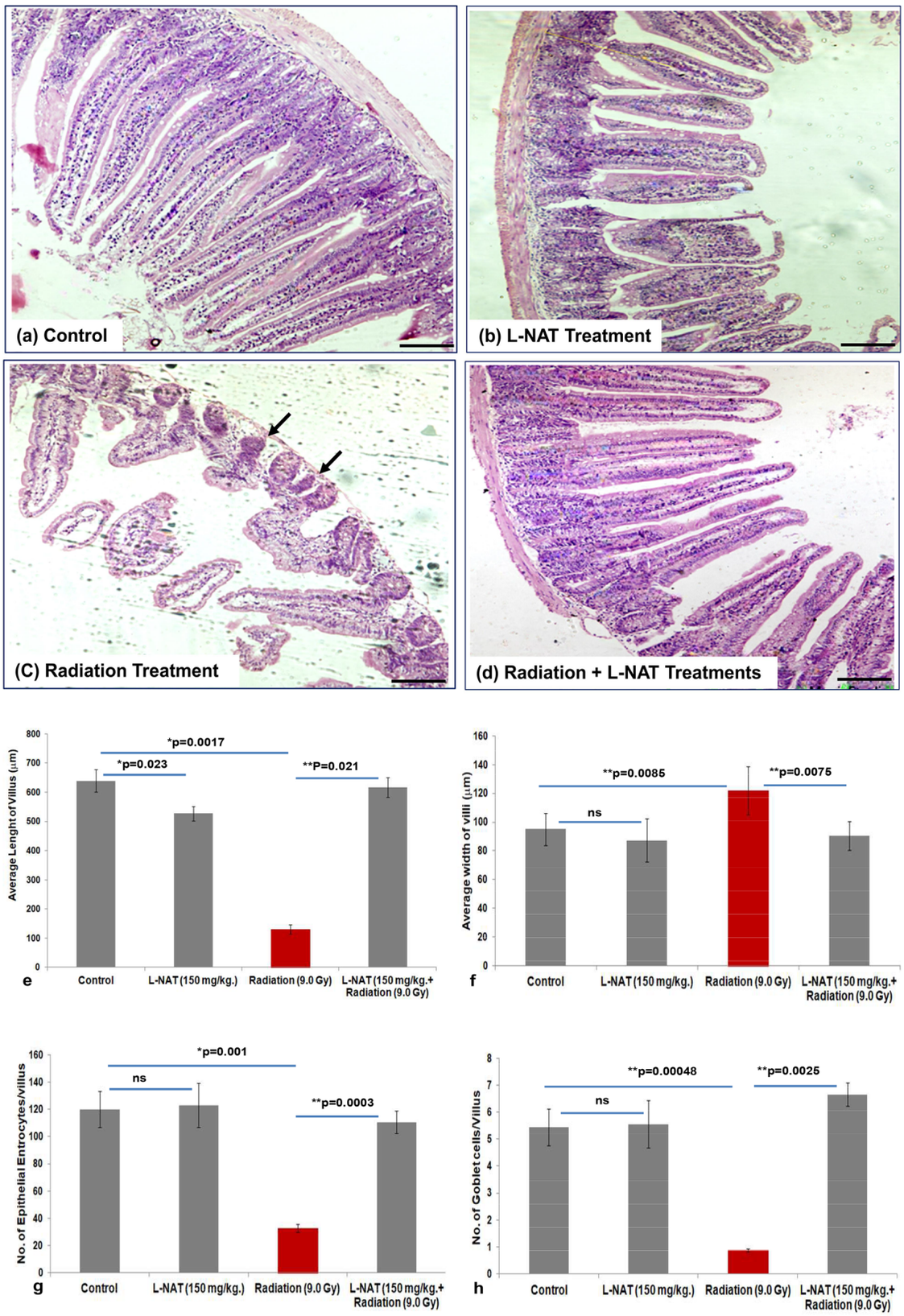

Figure 5. Determination of gastrointestinal system radioprotective activity of L-NAT at 14 day after radiation exposure. Normal cellular architecture of jejunum in control (a) and L-NAT treated (b) mice was observed. Radiation induced cellular structural damage (c), indicated by black arrow) and its protection by L-NAT pretreatment (d) was evaluated using microscopic observation at 10X magnification. Quantitative histological analysis of average length (e) and width (f), with, epithelial enterocytes (g) and goblet cells (h) per villus section was performed using NIS element software integrated with an automated microscope (Nikon Ti series, Japan). Total 5 slides were prepared in each experimental group and 4 tissues sections were analyzed per slides. Therefore total 20 tissue sections were quantitatively analyzed per experimental groups at day 14 time point. Same experiment was repeated three times. The standard deviation among the experimental groups was calculated as mean ± SD. Statistical significance of variance was also calculated using one-way ANOVA with Turkey test. The p value <0.05 was considered significant among the experimental group's comparison. ns; non-significant. Scale bar; 100 µm.

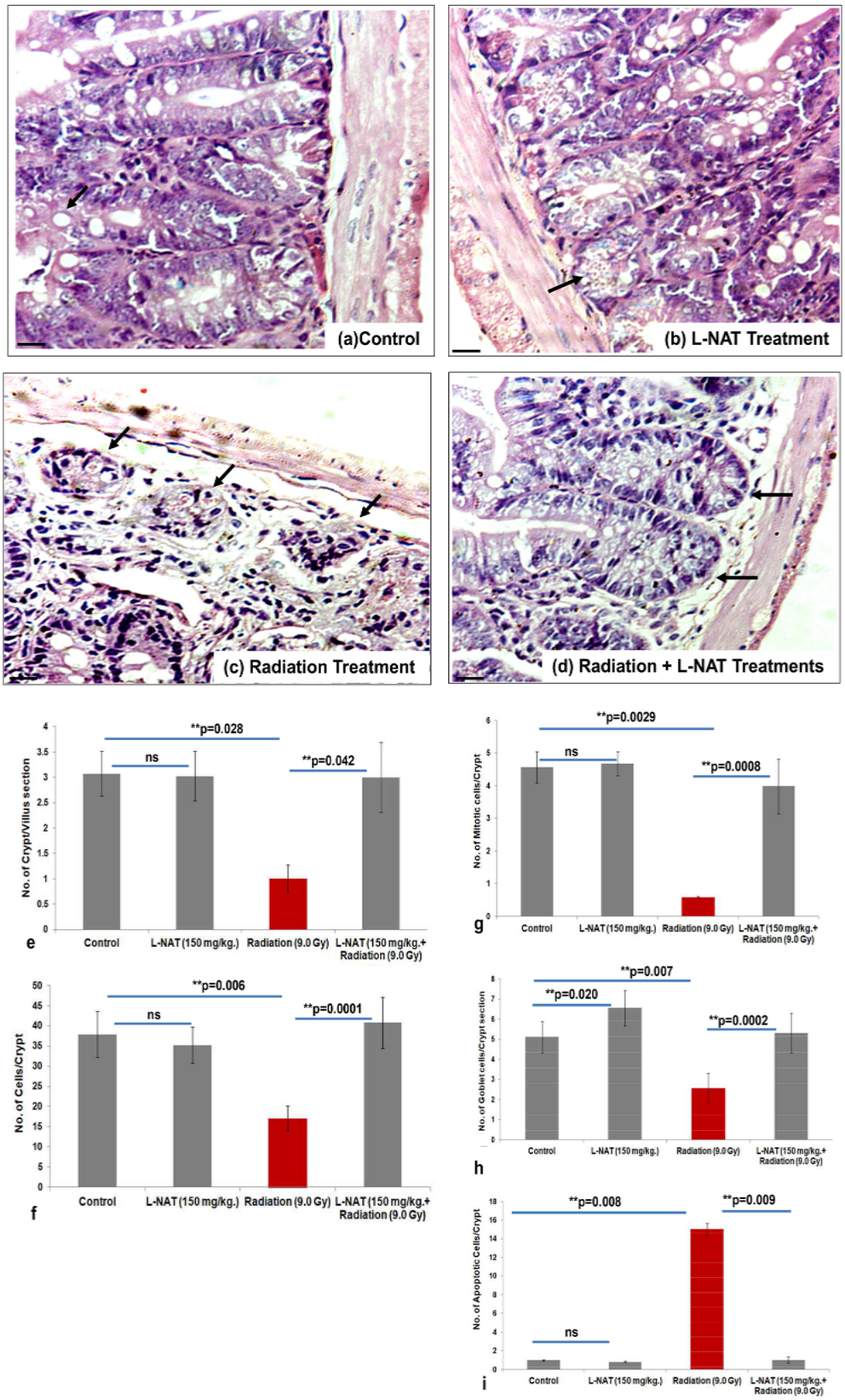

Figure 6. Radiation induced intestinal crypt cells degeneration and its protection by L-NAT pretreatment in irradiated mice at 14 day after radiation exposure. Normal crypt cells morphology was observed in control (a) and L-NAT treated (b) mice. Intestinal crypt cells morphological alterations and degenerative changes (c; indicated by black arrow) induced by gamma radiation and its protection by L-NAT pretreatment (d) were recorded under motorized microscopic (Nikon Ti-E) observations at 40X magnification. Quantitative analysis of intestinal crypt cells degeneration in terms of number of crypts per villus section (e), number of cells per crypt (f), number of mitotic cells per crypt (g), number of goblet cells per crypt section (h) and number of apoptotic cells per crypt (i) was performed using NIS element software integrated with an automated microscope (Nikon Ti series, Japan). Standard deviation calculated was expressed as mean ± SD. Significance of variance (p-value) $p < .05$ was considered significant. Significant of variance (p value) among the experimental groups was represented in within figure (e-i). ns; non-significant. Scale bar; 10 µm.

increase (p = .009; ~12-fold) in apoptotic cells numbers/crypt was observed with irradiated mice that were not pretreated with L-NAT compared to the irradiated mice that were pretreated with L-NAT (Figure 6i). These findings clearly suggest that L-NAT pretreatment significantly inhibits crypt stem cell death in irradiated mice and thus contribute to maintaining intestinal cellular homeostasis.

Influence of L-NAT pretreatment on intestinal crypts stem cell markers expression in the jejunum of irradiated mice

Significant reduction in Lgr-5, Msi-1, Bmi-1 and Dclk-1 intestinal stem cell markers expression was observed in the small intestine of irradiated mice at all tested time periods (Day1-7). However, maximum reduction (p < .05) in Lgr-5, MSi-1, Bmi-1 and Dclk-1 expressions was observed at day 3 and 5 compared to the respective untreated controls (Figure 7). In contrast, as a result of L-NAT pretreatment to irradiated mice, significant (p < .05) restoration of Lgr-5, Msi-1, Bmi-1, and Dclk-1 expressions was evident at all tested time periods (Day 1-7) compared to irradiated mice that not pretreated with L-NAT (Figure 7). These results clearly suggested that L-NAT pretreatment to irradiated mice was a contributory factor to preserving intestinal crypt stem cells from radiation-induced death.

Evaluation of hematopoietic system radioprotection offered by L-NAT pretreatment

Radioprotective effect of L-NAT on hematopoietic system was evaluated using histopathology of the femur bone LS section. The histological observations demonstrated severe suppression of erythropoiesis and myelopoiesis in the bone marrow of irradiated mice at day 14 (Figure 8c). While L-NAT pretreatment to irradiated mice provides significant recovery in the bone marrow cellularity compared to only irradiated mice that were not pretreated with L-NAT (Figure 8d). L-NAT pretreatment protects myeloblast, erythroblast and osteoblast of the irradiated mice in a time-dependent manner (data of 3 and 7 days not shown). L-NAT pretreatment to irradiated mice significantly preserves erythroblast, myloblast, and megakaryote(s) and thus provides comprehensive protection against gamma radiation induced immune suppression (Figure 8a,b,c,d).

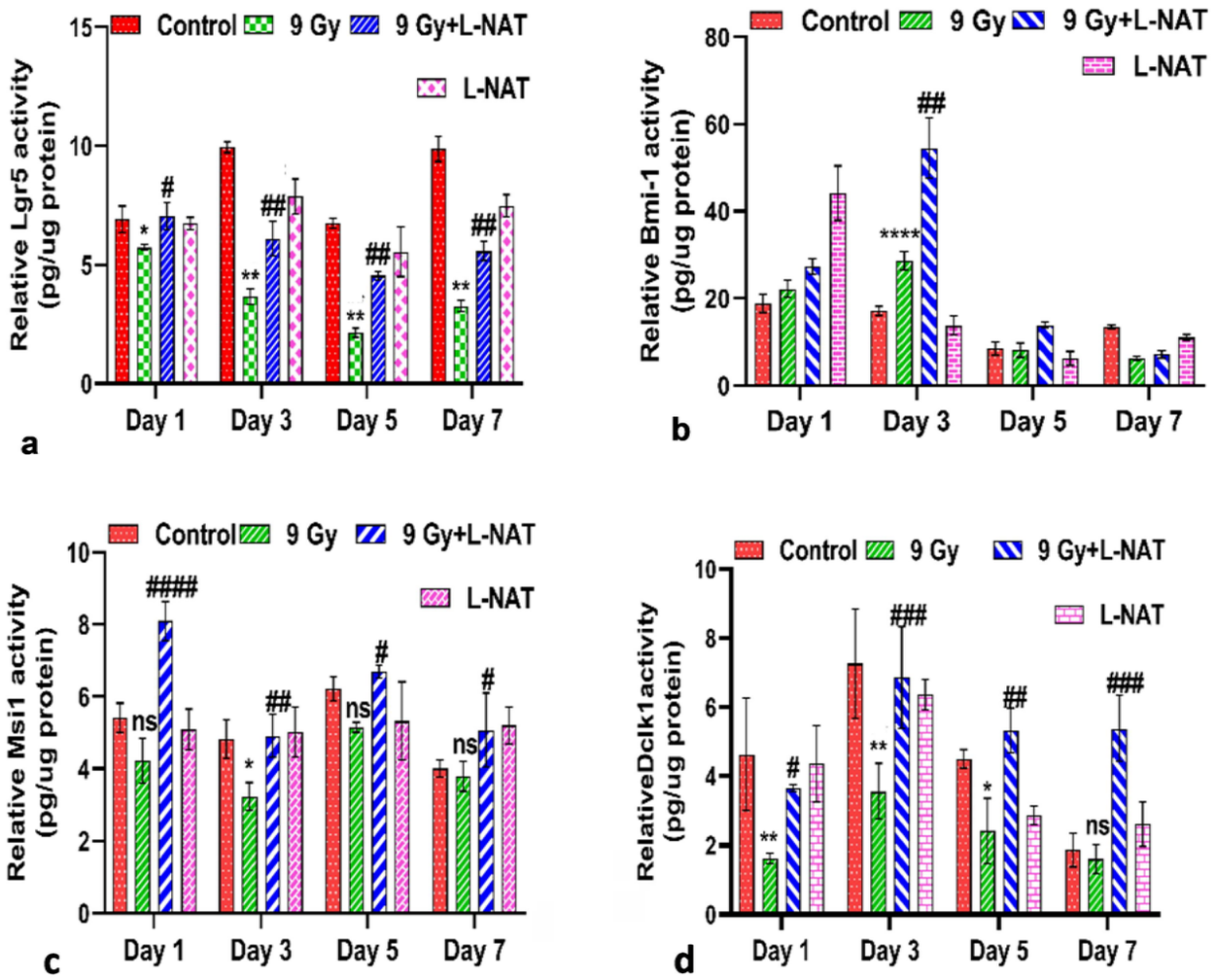

Figure 7. Protective effect of L-NAT on intestinal stem cells marker Lgr-5 (a), Bmi-1 (b), Msi-1 (c), and Dclk-1 (d) proteins expressions in small intestine (jejunum) of the irradiated **(9.0 Gy) mice.** Standard deviation calculated was expressed as mean ± SD. Significance of variation was represented as: Radiation treatment Vs control, *$p \leq 0.05$, **$p \leq 0.01$; L-NAT treatment + radiation treatment Vs radiation treatment, ****p < .0001, #p < .05, ##p < .01, ###p < .001, ####p < .0001; ns; nonsignificant.

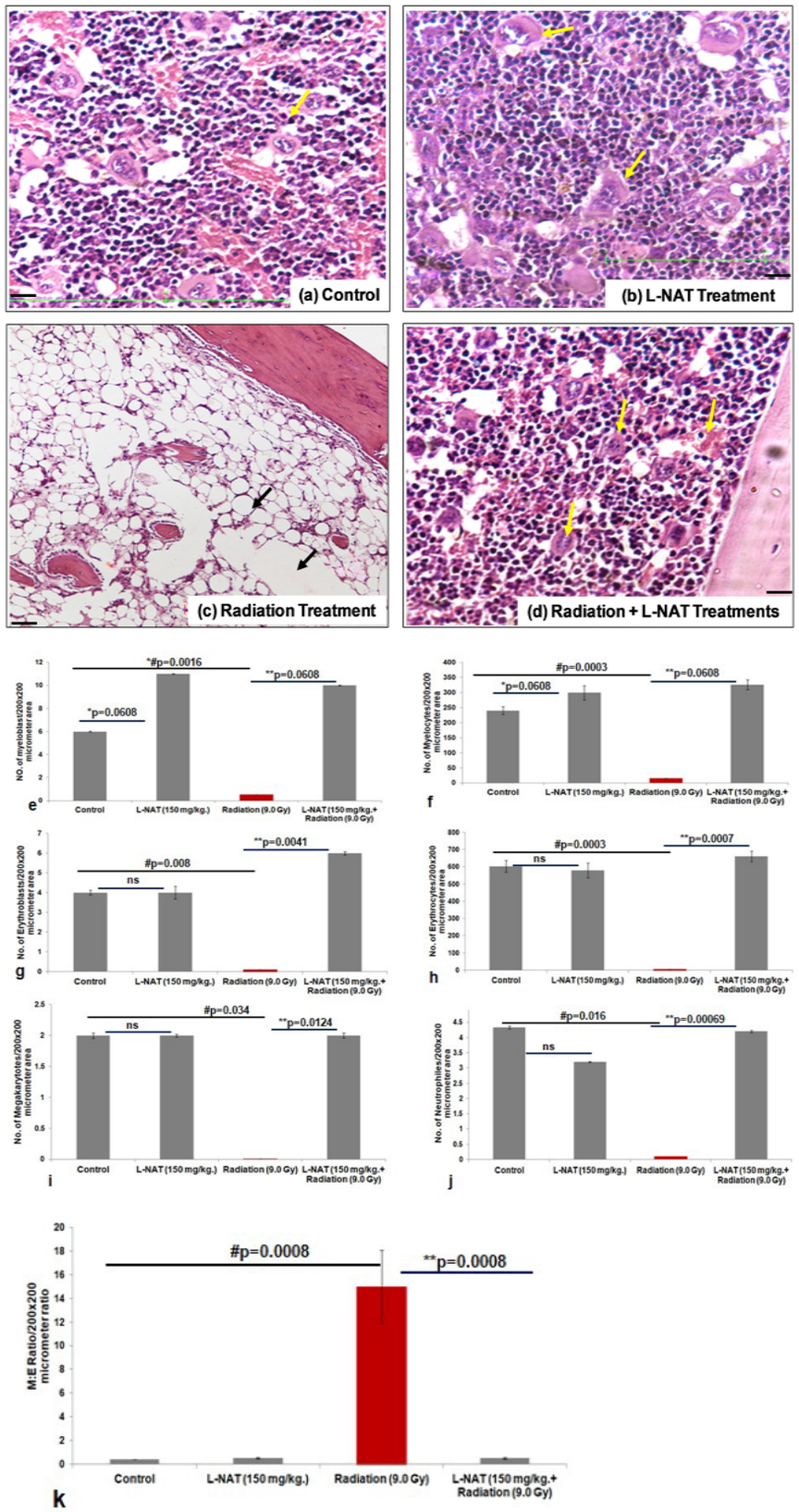

Figure 8. Radioprotective effect of L-NAT on hematopoietic system of irradiated mice. Bone marrow cellularity and its histological degenerative changes induced by gamma irradiation were analyzed and compared within different experimental groups using motorized microscopic (Nikon Ti-E) at 40X magnification. Yellow arrow represented the cellular integrity and architecture of myeloblast, megakaryote(s) and erythroblast cells (a, b, d) while, black arrow indicated the complete loss of bone marrow cellularity at day 14 after irradiation in the radiation control group of mice (c). Quantitative analysis of number of myeloblast (e), myelocytes (f), erythroblast (g), erythrocytes (h), megakaryote(s) (i), neutrophils (j) and M:E ratio (k) was performed in randomly selected multiple areas (200x200µm) of the slides using NIS element software integrated with a motorized microscope (Nikon-Ti-E). Standard deviation calculated was expressed as mean ± SD. Significance of variance (p-value) $p < .05$ was considered significant. Significant of variance (p value) calculated among the experimental groups was represented within figure (e-k). ns; non-significant. Scale bar; 10 µm.

Quantitative analysis of cellular architecture of bone marrow in irradiated and L-NAT pretreated mice

Quantitative analysis of bone marrow cellular architecture was performed using an automated motorized microscope. Observations demonstrated significant reduction in the number of myeloblast (p = .0016), myelocytes (p = .0003), erythroblasts (p = .008), erythrocytes (p = .0003), megakaryote(s) (p = .034), and neutrophiles (p = .016) in the bone marrow of irradiated mice that were not pretreated with L-NAT compared to untreated control at 14 day post treatment period (Figure 8e-k). As the result of L-NAT pretreatment to the irradiated mice, the number of myeloblast (~10-fold; p = .006), myelocytes (~13-fold; p = .006), erythroblasts (~6-fold; p = .004), erythrocytes (~100 fold; p = .0007), megakaryote(s) (~2-fold; p = .01), and neutrophils (~4-fold; p = .0006) was found to significantly increased as compared to the irradiated mice that not pretreated with L-NAT (Figure 8e-j). Interestingly, a high M:E ratio was observed with irradiated animals as compared to any other treatment groups (Figure 8k). These findings clearly suggest that L-NAT pretreatment significantly inhibits radiation induced myelopoiesis and erythropoiesis in irradiated mice and thus significantly ameliorate radiation induced immune-suppression.

Radioprotection to male reproductive system of the irradiated mice by L-NAT pretreatment

Reproductive system protection against gamma radiation (8 Gy) was studied using qualitative and quantitative testis histological analysis. Significant radiation induced cellular damage was observed in the testis of irradiated mice from day 7 to day 35. Clear deformation of seminiferous tubules, increase of tubule width, loss of primary and secondary spermatogonia, spermatatocytes and spermatids was evident in the irradiated (8 Gy) mice testis at all tested time points. On the other hand, compared to only irradiated mice, significant protection to seminiferous tubules' cellularity, improved number of primary and secondary spermatogonia, spermatocytes, and spermatids were observed in the irradiated mice that pretreated with L-NAT. Furthermore, compared to irradiated controls, well differentiated luminal area, tubule volume, spermatogonial cell population and well-organized spermatids were observed in L-NAT pretreated (-2h) and then irradiated mice (Figure 9a–p). These results clearly suggest the radioprotective potential of L-NAT toward germinal stem cells of seminiferous tubules.

Quantitative analysis of germinal cell types spermatogonia and spermatocytes in irradiated mice in presence and absence of L-NAT pretreatment

To evaluate the radioprotective potential of L-NAT toward the male reproductive system of mice, quantitative analysis of seminiferous tubules' histology was carried out on day 7-35 after gamma radiation and L-NAT pretreatments. Results of the study revealed significant reduction (>3-fold) in spermatogonia type-B and spermatocytes (>3-fold) per seminiferous tubules in both right and left testis as compared to untreated control at day 35 (Table-1). However, as the result of L-NAT pretreatment to irradiated mice, the number of spermatogonia type-B [(1.52-fold (R); 1.46-fold (L)] and spermatocytes [(1.64-fold (R); 1.61-fold (L)] per seminiferous tubules was found improved significantly (p < .05) as compared to irradiated mice that not pretreated with L-NAT. These finding clearly demonstrate germinal cell population protection ability of the L-NAT against radiation induced damage in male reproductive system (Table 1).

L-NAT radioprotective activity evaluation using NHPs model

Radioprotective activity of L-NAT was evaluated in Rhesus Macaque against 6.5 Gy gamma radiation. The results of the study revealed 100% whole body survival with the irradiated NHPs (Male + Female) that pretreated with L-NAT (37.5 mg/Kg, b.wt.im) compared to only 25% survival (Figure 10) with irradiated (6.5 Gy) NHPs that were not pretreated with L-NAT within 60 days post irradiation period. No supportive care was provided to any group of NHPs. The survival data was also supported by the hematology, biochemistry, organ function tests.

Hematology analysis in irradiated Rhesus Macaque after NAT pretreatment

As the result of whole-body gamma radiation (6.5 Gy) exposure, significant decrease in hemoglobin, RBCs, total leucocytes, lymphocytes, neutrophils and platelets counts were observed at day 2 and subsequent times and continuously remained at lower levels even at on day 30 (Figure 11a–g), compared to their respective control level at zero time (level before the treatment). Out of four animals (Male n = 2 and female n = 2), three animals [(number 654 (M), 518 (F) and 542 (F)] did not survive beyond day 20 post treatment period, thus no further analysis was carried out. Single irradiated animals [(No. 650 (M)] survived was demonstrated recovery in hematological parameters except lymphocytes % after day 30 post irradiation period (Figure 11a–g). Whereas, irradiated animals that pretreated with L-NAT (i.e. male no. 656, 631 & female animals no. 565 515) were demonstrated significant recovery in hematological parameters after day 14-20 post treatment periods. The hematological analysis revealed significant recovery in all hematology parameters within 7 months in all irradiated NHPs that pretreated with L-NAT, suggest hematopoietic system radioprotective effect of L-NAT.

Blood biochemistry analysis in irradiated NHPs after L-NAT pretreatment

To study the effect of gamma irradiation on kidney and liver functions, blood biochemical tests were performed. Urea, blood urea nitrogen (BUN), creatinine, uric acid, total proteins, albumin- globulin ratio, total phosphorus, calcium, sodium, potassium and chloride concentrations

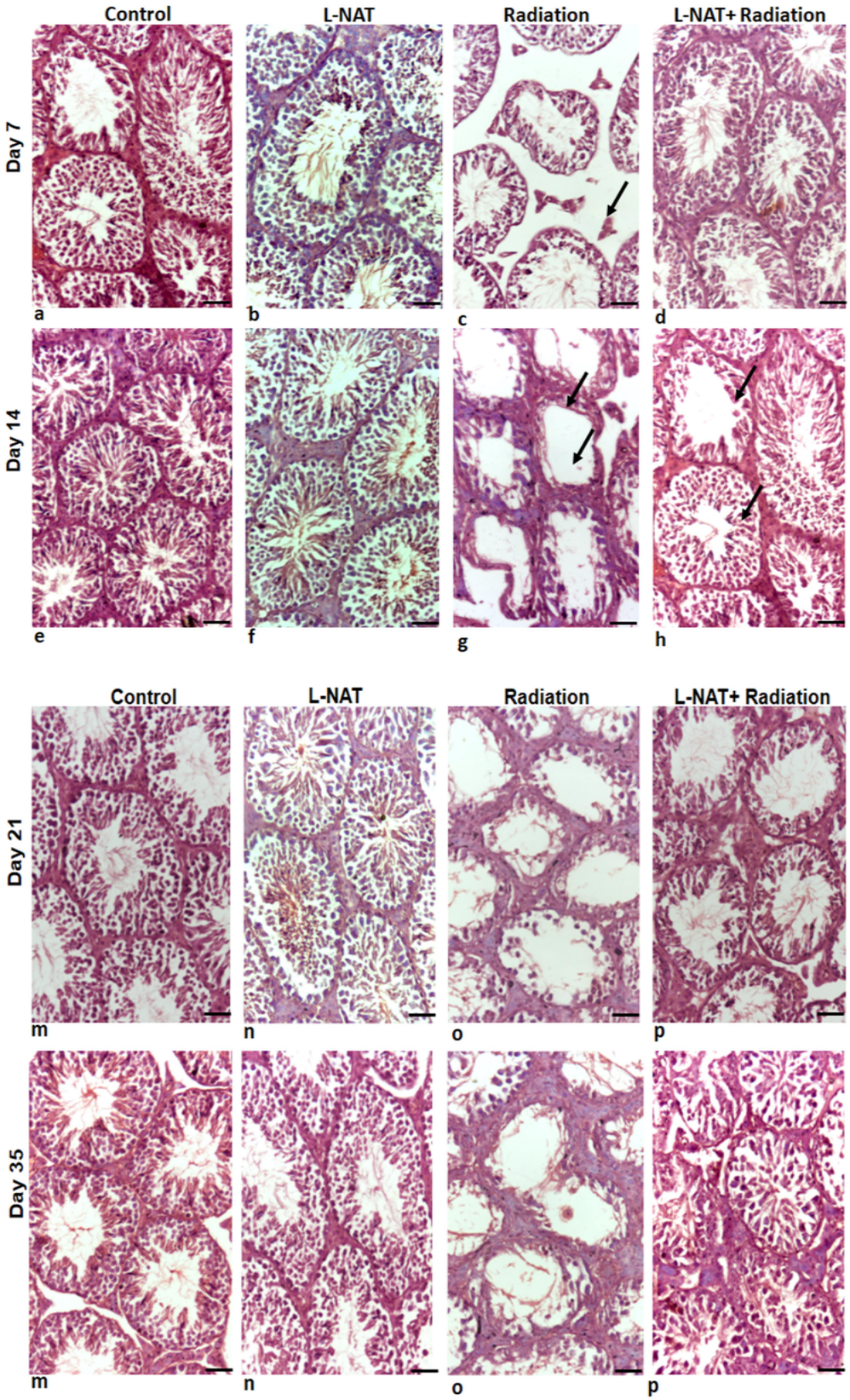

Figure 9. Radioprotection offered by L-NAT to male reproductive system of irradiated mice. Histological degenerative changes such as deformation of seminiferous tubules, increase of tubule width, loss of spermatogonia, spermatatocytes and spermatids (indicated by black arrow) appeared in the seminiferous tubules of irradiated (8 Gy) mice were recorded and compared with the irradiated mice that pretreated with L-NAT at 40X magnification using motorized microscope (Nikon Ti-E) at 7 (a-d), 14 (e-h) and 21 (i-l), and 35 (m-p) day post treatment period. Scale bar; 10 µm.

was estimated. Urea concentration in irradiated animals was found in increasing order at 10 (p = .038) to 14 (*p* = .009) day. At subsequent time, single alive animal (irradiated) showed high urea concentration (83.3 mg/dL) at 30 days compared to control (31.3 mg/dL). The urea concentration estimated at 7 months later of irradiation in single alive irradiated animal was found to be 112 mg/dL (Figure 12a). Whereas, urea concentration in the blood of irradiated animals that were pretreated with L-NAT, increased up to 10 days and gets normalized in subsequent times (Figure 12a). No significant difference in BUN was reported in irradiated NHPs that pretreated with L-NAT at any time period compared to their respective control (Figure 12b). However, higher concentration of BUN was report in single survived irradiated animal beyond 20 days (Figure 12b). No significant perturbation in total protein concentration was observed in irradiated NHPs irrespective of their L-NAT pretreatment up to 20 days. However, noticeable reduction in total proteins concentration observed with irradiated NHPs that not pretreated with L-NAT compared to NHPs that were pretreated with L-NAT (Figure 12f). Albumin-globulin ratio was found to be decreased in irradiated NHPs irrespective with their L-NAT pretreatment upto 20 day, however, a recovery in albumin:globulin ratio was reported in irradiated NHPs that pretreated with L-NAT compared to the NHP that did not pretreated with L-NAT at day 30 and 7 months later (Figure 12 g). No significant difference in creatinine, uric acid, total calcium, phosphorus, sodium, potassium and chloride was observed with the NHPs of any experimental groups (Figure 12c,d,h,i,j,kl).

To evaluate the effect of gamma irradiation on liver enzymes, Serum glutamic-oxaloacetic transaminase (SGOT), Serum glutamic pyruvic transaminase (SGPT), Gamma-glutamyl transpeptidase (GGTP) and alkaline phosphatase concentration in the blood of NHPs were estimated. Significant induction in SGOT, SGPT and alkaline phosphatase was observed at day 2 time period in irradiated NHPs irrespective of their L-NAT pretreatment (Figure 13,a,b,d). The expression of SGOT and SGPT was found to return at their normal level within 20 day post irradiation period in both sets of experimental animals, however, expression of alkaline phosphatase remains high at 30 days with irradiated NHPs that were not pretreated with L-NAT compared to irradiated NHPs that were pretreated with L-NAT

Table 1. Quantitative analysis of germinal cells types i.e. spermatogonia and spermatocytes in irradiated mice with or without L-NAT pretreatment at day 35 post-treatment period.

Treatment group	Germinal cell types			
	Number of spermatogonia-b/ seminiferous tubules at Day 35		Number of Spermatocytes/ seminiferous tubules at Day 35	
	Right testis	Left testis	Right testis	Left testis
Control	13.5 ± 1.82	12.9 ± 1.91	64.1 ± 4.43	62.5 ± 3.24
L-NAT	12.2 ± 2.12	12.2 ± 1.61	61.0 ± 3.96	59.1 ± 6.29
Radiation	4.2 ± 1.17	4.7 ± 0.97	22.8 ± 3.10	24.2 ± 3.13
L-NAT+ Radiation	6.4 ± 1.37	6.9 ± 1.41	37.5 ± 3.27	39.0 ± 5.65
P Value	L-NAT Vs L-NAT+ Radiation p = 0.044	L-NAT Vs L-NAT+ Radiation p = 0.041	L-NAT Vs L-NAT+ Radiation p = 0.037	L-NAT Vs L-NAT+ Radiation p = 0.034

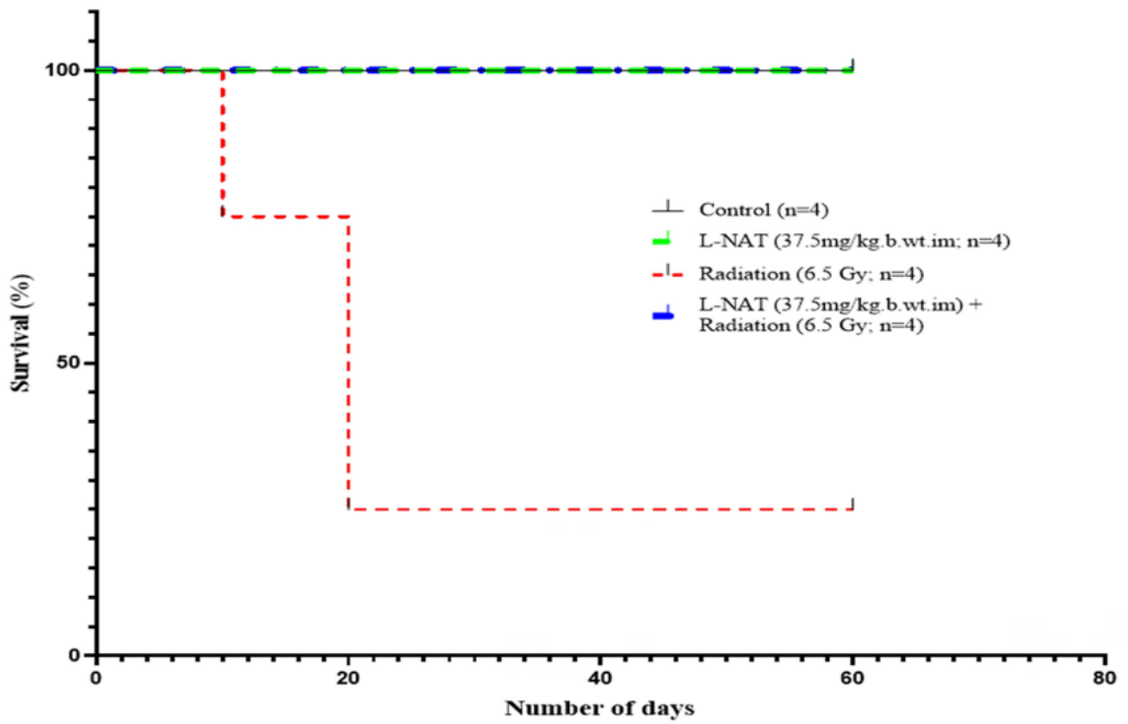

Figure 10. L-NAT radioprotective activity determination in NHP. Rhesus macaque (n = 4) were administered with L-NAT (37.5 mg/Kg, b.wt.im) formulation 2h before whole body irradiation (6.5 Gy), and 60 days survival (%) was reported and comapred with the irradiated (6.5 Gy) macaque (n = 4) that were not pretreated with L-NAT formulation. Each experimental groups having 4 animals (2 male and 2 female). The animals were strictly monitored for their food and water consumption, heamatology, blood biochemistry and general behavioral characteristics. No additional supportive care was provided to the animals of any experimental group.

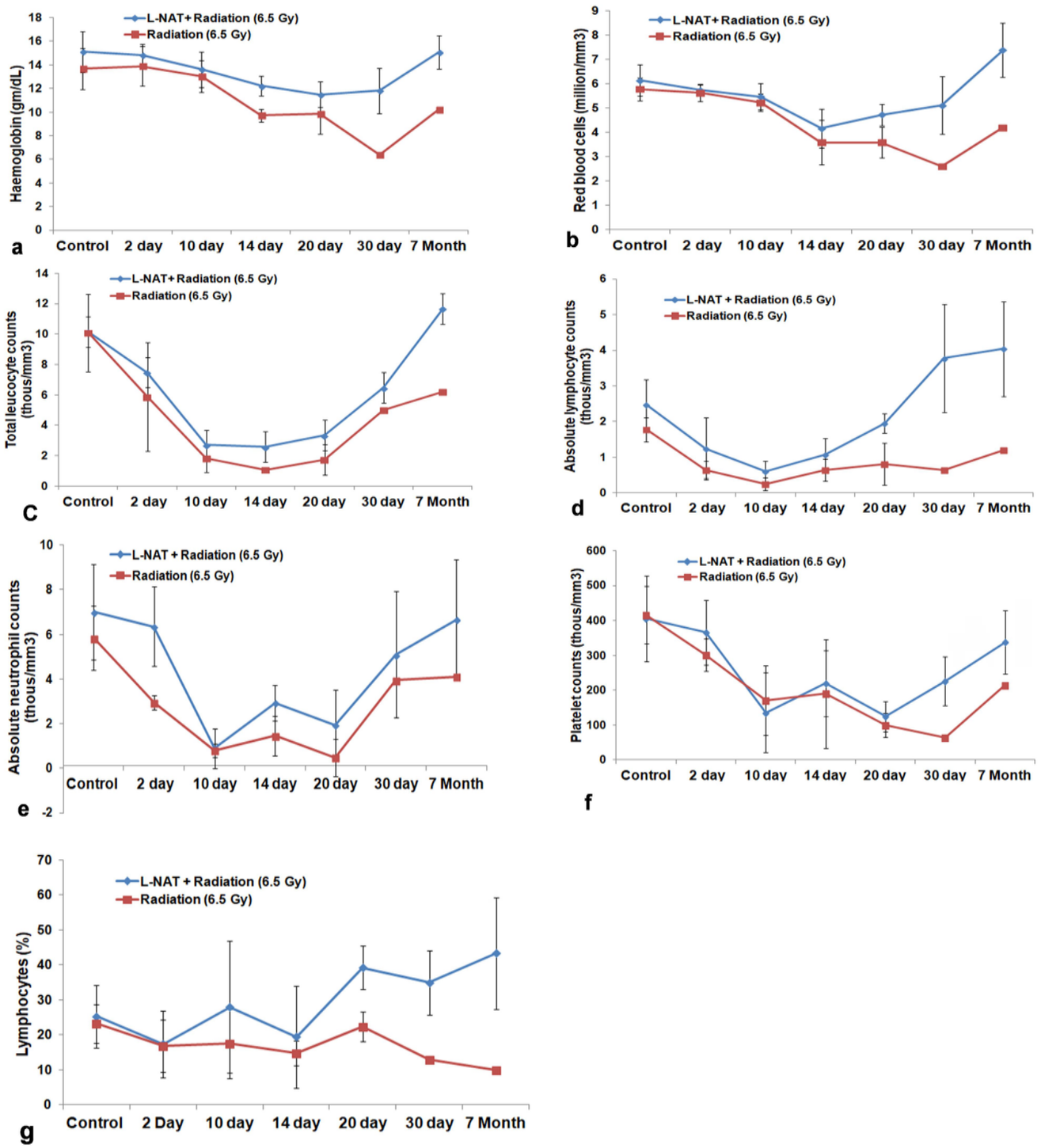

Figure 11. Hematological analysis of irradiated and L-NAT administered NHPs. Blood samples of NHPs of all treatment groups were collected at day 2, 10, 14, 20, 30 and 7 months periods and undertaken for hematological analysis. Hematological parameters such as hemoglobin (a), red blood cells (b), total leucocytes (c), absolute lymphocytes count (d), absolute neutrophils (e), platelets counts (f) and lymphocytes percentage (g) were reported using automated hematological analyzer and compared with the blood parameters of untreated control animals (i.e. 0 day; blood collected one day before radiation and L-NAT + radiation treatments). Data was presented as the means of hematology data of four animals (n = 4) in an experimental group at different time points. Standard deviation within the data of an experimental group (n = 4) was presented as ± SD. No supportive care was provided to group of animals. In irradiated NHPs that not pretreated with L-NAT, out of four, only one animal survived beyond 20 days post-irradiation periods, therefore, no standard deviation was calculated at 30 and 7 months' time points.

(Figure 12d). Although alkaline phosphatase was observed to return at their normal levels in 7 months in L-NAT pretreated plus irradiated NHPs, but it was remained at higher level in irradiated NHPs (single animal survived) even at 7 months later of irradiation. No significant perturbations in GGTP level were reported in irradiated NHPs irrespective their L-NAT pretreatment (Figure 13c) up to 30 days post irradiation period. However, level of GGTP was found higher in single survived irradiated animals at 7 months later of irradiation (Figure 13c).

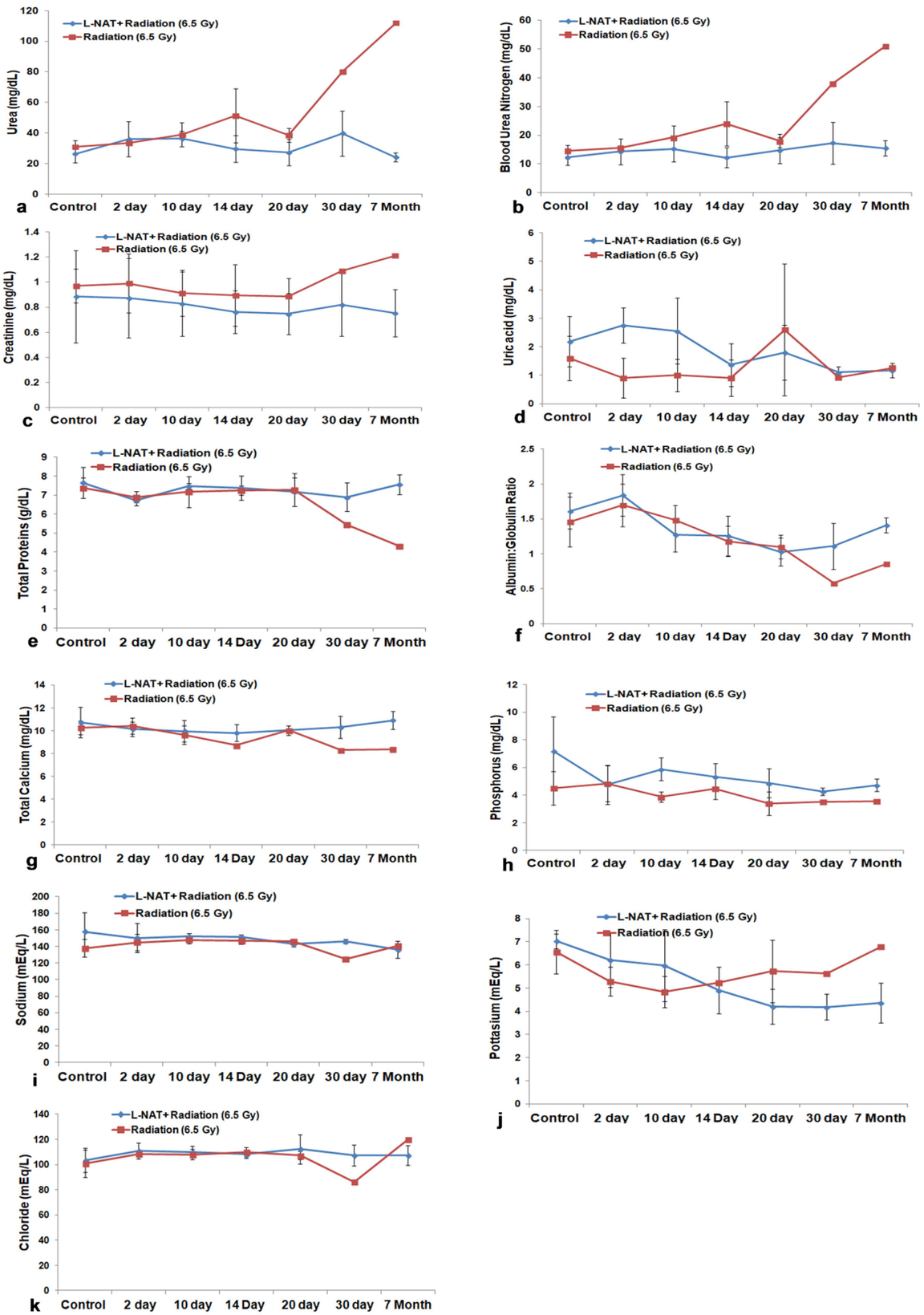

Figure 12. Kidney function test (KFT) analysis of irradiated and L-NAT administered NHPs. Blood samples of NHPs of all treatment groups were collected at day 2, 10, 14, 20, 30 and 7 months periods and undertaken for kidney function test. Kidney function tests parameters i.e. Urea (a), blood urea nitrogen (b), creatinine (c), uric acid (d), total protein concentration (e), albumin: globulin ratio (f), along with total calcium (g), phosphorus (h), sodium (i), potassium (j), and chloride (k) was performed using automatic blood biochemistry analyzer and compared with the KFT parameters of untreated control animals (i.e. 0 day; blood collected one day before radiation and L-NAT + radiation treatments). Data was presented as the means of data of four animals (n = 4) in an experimental group at different time points. Standard deviation in the data of an experimental group (n = 4) was presented as ± SD. No supportive care was provided to any group of animals. In irradiated NHPs that not pretreated with L-NAT, out of four, only one animal was survived beyond 20 day post irradiation periods, therefore, no standard deviation was calculated at 30 and 7 month time points.

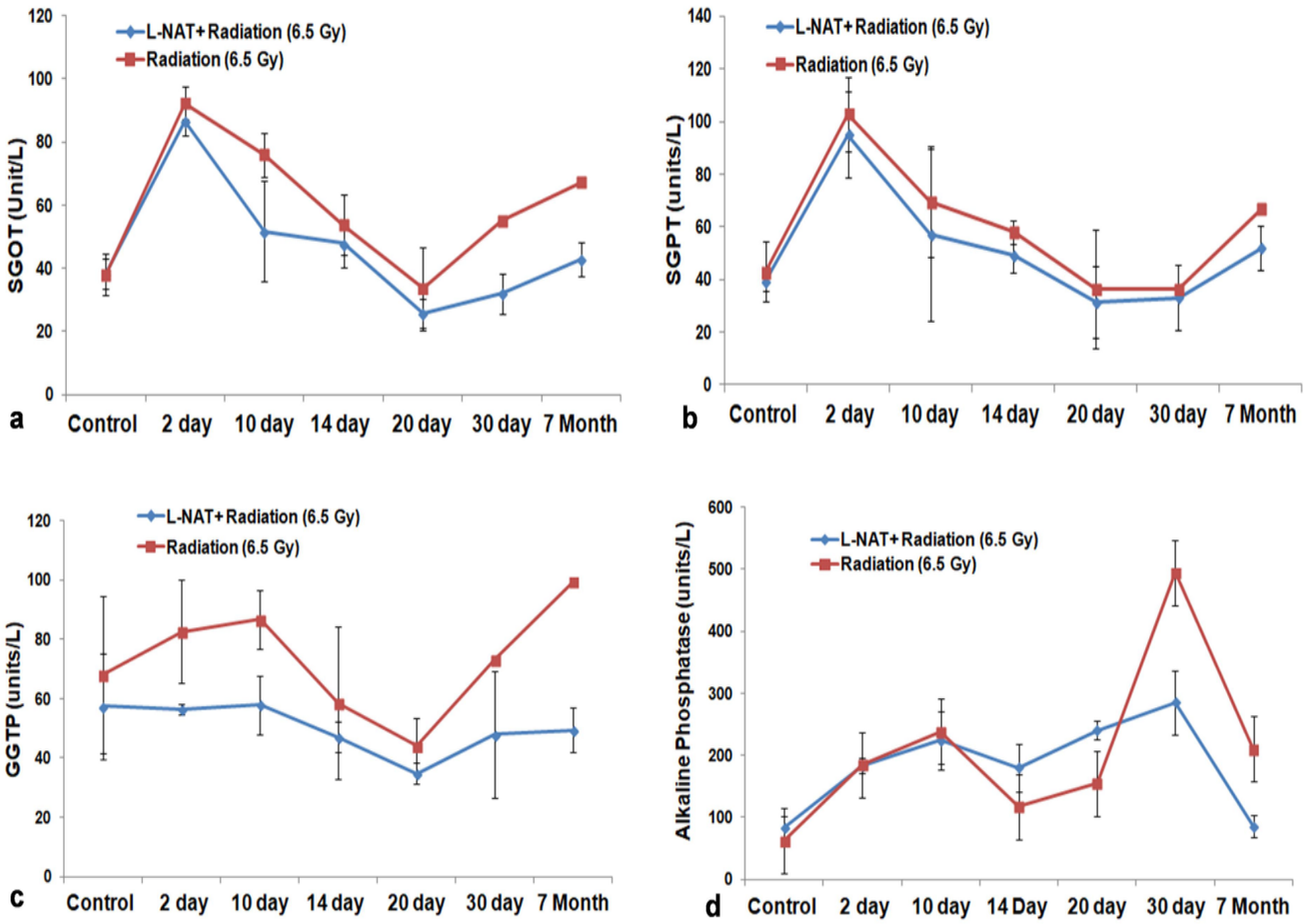

Figure 13. Liver function test (LFT) analysis of irradiated and L-NAT administered NHPs. Blood samples of NHPs of all treatment groups were collected at day 2, 10, 14, 20, 30 and 7 months periods and undertaken for liver function tests. LFT i.e. SGOT (a), SGPT (b), GGTP (c) and alkaline phosphatase (d) was performed using an automatic blood biochemistry analyzer and compared with the LFT parameters of untreated control animals (i.e. 0 day; blood collected one day before radiation and L-NAT + radiation treatments). Data was presented as the means of LFT parameters of four animals (n = 4) in an experimental group at different time points. Standard deviation in the data of an experimental group (n = 4) was presented as ± SD. No supportive care was provided to any group of animals. In irradiated NHPs that not pretreated with L-NAT, out of four, only one animal was survived beyond 20 days post-irradiation periods, therefore, no standard deviation was calculated at 30 and 7 month time points. SGOT; serum glutamic-oxaloacetic transaminase, SGPT; serum glutamic pyruvic transaminase, GGTP; gamma-glutamyl transpeptidase.

Radiation induced DNA damage and its protection by L-NAT pretreatment in irradiated NHPs

To evaluate the radiation-induced DNA damage and its amelioration by L-NAT pretreatment, blood samples of animals were collected just before and after radiation treatment with or without L-NAT administration, and an immediate alkaline comet assay was performed. The results of the study indicated massive DNA damage and nucleus swelling in the blood cells of irradiated NHPs that were not preinjected with L-NAT (Figure 14c). However, no such DNA damage was evident in the blood cells of irradiated NHPs that were preinjected with L-NAT (Figure 12d), though nucleus swelling was evident. No significant DNA damage was evident with the control and L-NAT-treated group of NHPs (Figure 14a,b). The present study clearly demonstrated the in vivo DNA protection ability of L-NAT against gamma radiation induced DNA damage in the blood cells.

Efficacy biomarker evaluation for L-NAT in NHP model

To evaluate the radioprotective efficacy biomarkers for L-NAT mediated radioprotection, animals (n = 4) were injected with L-NAT 1x (37.5 mg/kg), 2x (75 mg/kg) and 3x (112.5 mg/kg) escalating doses and after 2h (therapeutic window), blood was collected for cytokines, i.e. G-CSF, IL-6, IL-12, NFkB expression analysis. Results of the study demonstrated a dose dependent increase in G-CSF (beyond 2x dose) and IL-6 expressions at 2h post injection period (Figure 15a,b), suggested positive efficacy biomarkers for L-NAT mediated radioprotection in the NHP model. However, NFkB expression was found to decrease significantly (p = .021) at 1x dose of L-NAT and remain same at subsequent dosing (2-3x), suggesting a negative efficacy biomarker for L-NAT mediated radioprotection (Figure 15d). A significant (p = .0019) increase in IL-12 expression was also evident at 1x L-NAT concentration, whereas, at subsequent 2x and 3x L-NAT doses, IL-12 expressions were found to be decreased strongly (Figure 15c), suggesting IL-12 as an intermediate efficacy biomarker for the L-NAT mediated radioprotection in NHP model.

Discussion

Several radioprotective molecules have been evaluated for their radioprotective potential and at different stages of preclinical development (Singh et al. 2013; Malhotra et al. 2015;

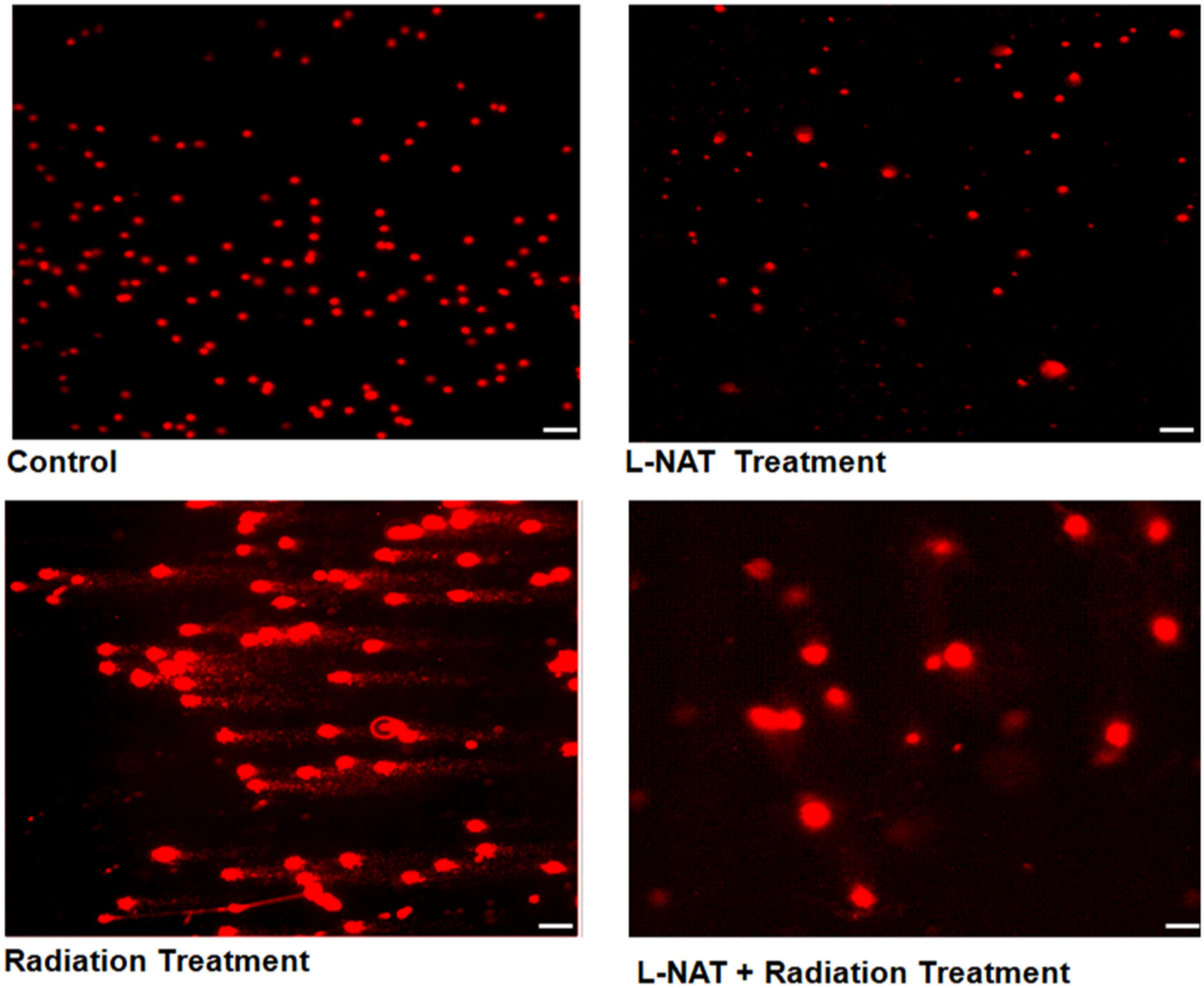

Figure 14. Evaluation of radiation-induced DNA damage in the blood cells of irradiated NHPs and its amelioration by L-NAT pretreatment. Blood samples of **NHPs of different experimental groups** were collected just from respective treatments and alkaline comet assay was performed. Slides were stained with ethidium bromide and observed under automated fluorescence motorized microscope (Nikon-Ti-E). The DNA comet tail in the blood cells collected from irradiated NHPs that were not pretreated with L-NAT was captured and compared with the DNA of the blood cells collected from irradiated NHPs that pretreated with L-NAT. Scale bar; 10 µm.

2018; Mun et al. 2018; Wickramasinghe et al. 2022; Darshana et al. 2023; Pratibha et al. 2023). L-NAT for the first time is being evaluated for its radioprotective activities by our group. Radioprotective activity of L-NAT was found to be supported by its outstanding free radical scavenging, oxidative stress minimizing, DNA and mitochondrial systems protection and calcium homeostasis maintenance in the cellular milieu (Lehnig et al. 2007; Li et al. 2015; Ravi et al. 2022; Darshana et al. 2023; Pratibha et al. 2023). The maximum survival of irradiated mice was achieved upon L-NAT pretreatment 2 h before irradiation (Figure 3). However, further increasing the time window (3 h) of L-NAT pretreatment led to a significant decrease in the survival (%) of irradiated mice compared to 2 h before L-NAT treatment. Effectiveness of L-NAT within a 1.5–2 h time window suggested its specific ADME characteristics, pharmacokinetics, and pharmacodynamic properties. Pharmacokinetics studies done (data not shown) suggested >90% elimination of L-NAT from the body of the mice within 4 h after intramuscular injection. These observations suggested that L-NAT may take 1.5–2 hours to achieve its effective concentration at systemic levels and modulate it at the biochemical and molecular level to produce radioprotective effects. However, a more focused study will be needed to confirm the molecular mechanism of L-NAT-mediated radioprotection.

The dose reduction factor (DRF) estimated for L-NAT radioprotective efficacy in mice to be 1.33 (Figure 4) that was found comparable with other advanced staged (IND status) radioprotective molecules i.e. amifostine (DRF 2.27), CBLB 502 (DRF 1.3 based on body wt. loss), alpha tocopherol (DRF 1.06-1.11), 5 AED (DRF 1.25), X-RAD (DRF 1.16), genestin (DRF 1.16) (Ghosh et al. 2009; Burdelya et al. 2012; Grace et al. 2012; Singh and Krishnan 2015; Landauer et al. 2019), provided a strong support to the radioprotective efficacy of L-NAT. It is interesting to mentioned that DRF of amifostine drop from 2.7 to 1.2 at the dose that have minimized side effect (Singh et al. 2005).

Molecular docking study demonstrated common binding site of L-NAT and TRPV1 agonist capsaicin on TRPV1 receptor with binding energy −8.0 and 8.2 respectively

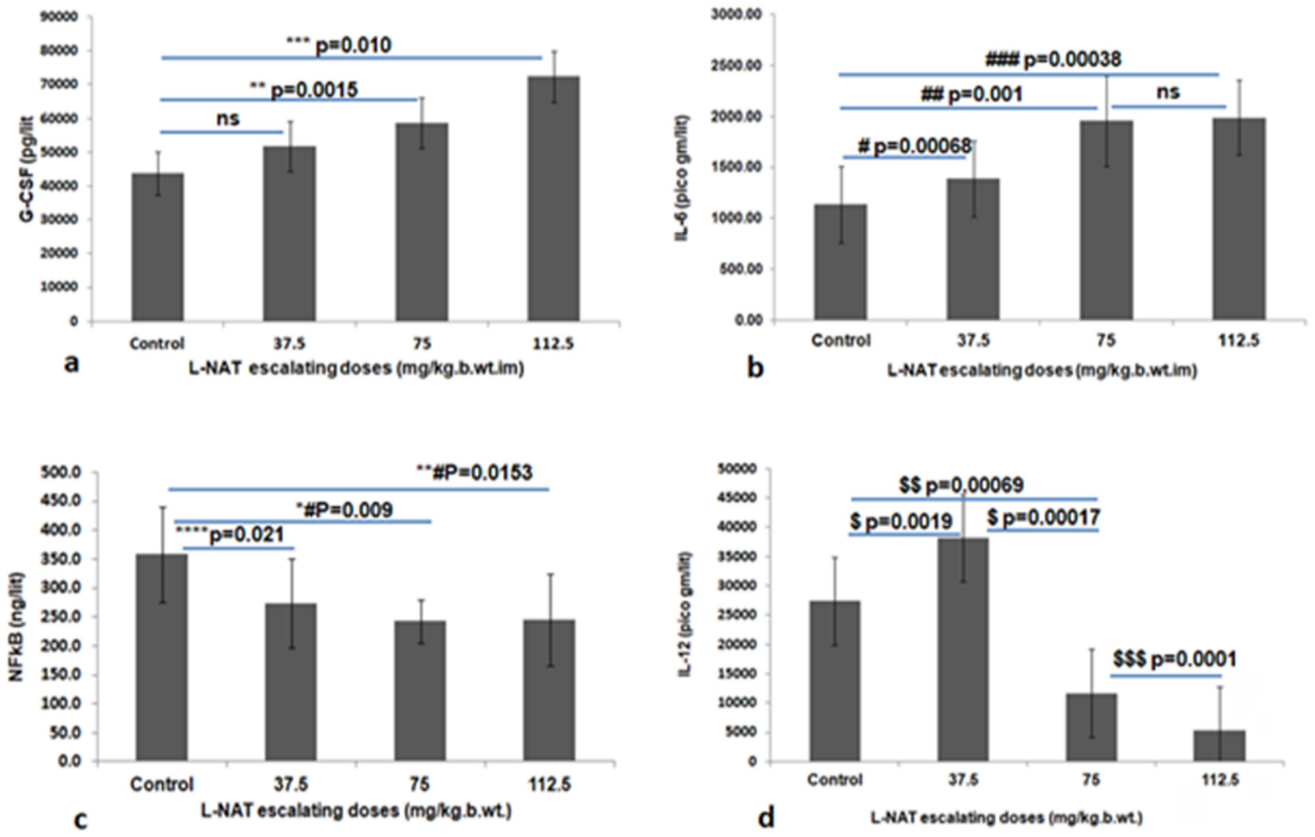

Figure 15. Radioprotective efficacy biomarkers expression analysis in the serum of NHPs after L-NAT escalating doses (1-3x) administration. NHPs were administered with escalating doses of L-NAT i.e. 1x (37.5 mg/kg; n = 4), 2x (75 mg/kg; n = 4) and 3x (112.5 mg/kg; n = 4). Blood samples were collected from all three experimental groups (1x, 2x and 3x) after 2h of L-NAT administration (im) and efficacy biomarker i.e. G-CSF (a), IL-6 (b), IL-12 (c), NFkB (d) analysis was performed using Elisa assay. The data was represented as the mean ± SD of the three individual animals in an experimental group. Significance of variance (*p*-value) $p < .05$ was considered significant. Each experimental group has 3 animals (n = 4).

(Figure 1a,b). Interestingly, capsaicin treatment induced substance P levels, while, L-NAT treatment inhibits it in the small intestine and serum of the mice (Figure 1c, d). These findings suggested a close competition between capsaicin and L-NAT to bind with the TRPV1 receptor. However, both ligands induce relatively opposite effects in the system. L-NAT pretreatment also inhibits capsaicin or gamma radiation induced substance P expression in the serum and small intestine of the mice and thus may act as a TRPV1 antagonist. Amelioration of radiation induced substance P [a known neurokinin-1 receptor; (NK-1R) agonist] release in the intestinal and circulatory system by L-NAT pretreatment (Figure 1c,d), may inhibit NK-1R activation and thus block systemic inflammation and cell death as reported earlier (Bowden et al. 1994; Tang et al. 2007; Pratibha et al. 2023; Teodoro et al., 2023) providing gaining support to the present study. Capsaicin, ethanol and radiation are known to induce substance P release from the sensory nerve ending by activation of a TRPV1 receptor. Previous reports demonstrated TRPV1 activation release substance P that led to enhanced Ca^{+} influx inside the cytoplasm that stimulates mitochondrial membrane hyperpolarization along with inflammatory response, oxidative stress and apoptosis (Gazzieri et al. 2007; Waning et al. 2007; Okada et al. 2011; Vinuesa et al. 2012; Abe et al. 2013; Masumoto et al. 2013; Wu et al. 2014; Pecze et al. 2016; Gouin et al. 2017; Fonseca et al. 2018; Li et al. 2019) in the cellular milieu. Thus, amelioration of substance P release via L-NAT pretreatment (Figure 1c,d) to irradiated mice inactivate TRPV1 (Figure 1c,d), and thus may help to remain NK-1R inactivated resulted systemic inflammation and death inhibition in irradiate mice. Supporting earlier reports (Bowden et al. 1994; Tang et al. 2007; Teodoro et al. 2013) providing gain support to present study. Apart from that, TRPV1 overactivation is also known to inhibit cell proliferation by suppressing the phosphorylation of epidermal growth factor receptor (EGFR) (de Jong et al. 2014). Likewise, proliferation of human melanoma A2058, A375 cells, pancreatic cancer PANC-1 cells and human skin carcinoma A431 cells were also reported to be inhibited after TRPV1 overexpression due to apoptosis induction (Bode et al. 2009; Yang et al. 2018; Huang et al. 2020; Li et al. 2021). All these studies strongly suggest that TRPV1 overexpression may promote cell death via enhancing oxidative stress, inflammation and apoptosis and thus promote radiosensitivity in biological systems. Therefore, amelioration of TRPV1 overexpression may protect the cells against radiation-induced cell death. To further evaluate the radioprotective activities of L-NAT in radiosensitivity systems, i.e.hematopoietic, gastrointestinal and male reproductive systems, qualitative and quantitative histopathological analysis was carried out. With complete agreement with the earlier reports (Nicholas 2002; Lu et al. 2020; Fooladi et al. 2022), almost complete abolition of myeloblasts, myelocytes, erythroblasts and erythrocytes, and megakaryote(s) was

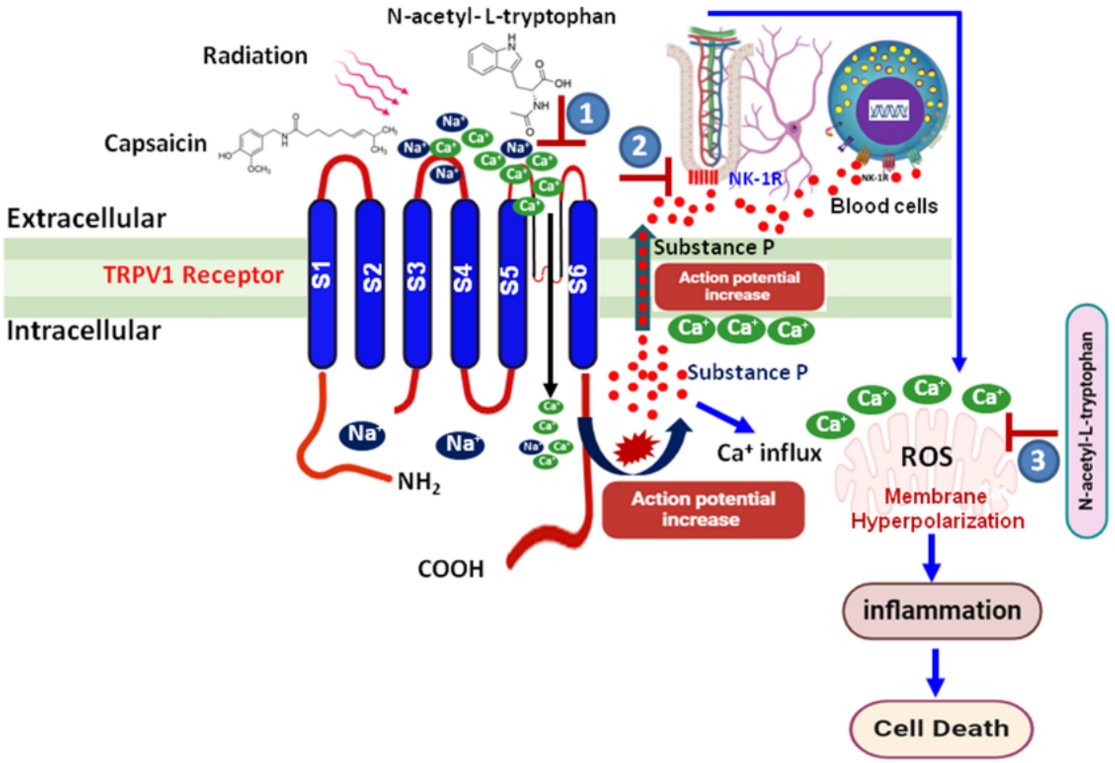

Figure 16. Schematic representation of TRPV1 receptor involvement in radiation-induced substance P release, Ca + inflex induction, mitochondrial membrane hyperpolarization leading to inflammation, and death in irradiated animals. On the other hand, L-NAT-mediated TRPV1 receptor inactivation inhibits Ca^{+} influx in cells. This phenomenon may inhibit several TRPV1 receptor descendent activities including Ca + influx-mediated cell membrane hyperpolarization and subsequent substance P release from sensory neurons resulting neurokinin-1 receptor antagonism leading to radiation-induced inflammatory response inhibition. Simultaneously, as Ca + influx was inhibited by L-NAT pretreatment, mitochondrial membrane hyperpolarization was also inhibited which may also contribute to inflammation and apoptosis inhibition and thus contribute to radioprotection in irradiated mice. ⊢; represents inactivation of TRPVA receptor (1), neurokinin-1 receptor inactivation (2) and mitochondrial membrane hyperpolarization inhibition (3), as prime molecular targets of L-NAT in cellular milieu.

observed within day 14 post irradiation period in the bone marrow of irradiated mice that not pretreated with L-NAT (Figure 8c, e-j). In contrast, well-preserved cellular compositions with distinct and maintained myeloblasts, myelocytes, erythroblasts and erythrocytes, megakaryote(s) and neutrophils were evident with irradiated mice that pretreated with L-NAT (Figure 8d,e–j). These observations clearly suggested that L-NAT pretreatment significantly ameliorates radiation induced immune-suppression by preserving myelopoisis, and erythropoiesis in the irradiated mice and thus significantly contributes to the survival of the irradiated mice. Similar observations were also reported with other radioprotective molecules under preclinical investigations, i.e. CBLB-502, 5-AED, KMRC001, alpha-tocopherol, NATG (Satyamitra et al. 2011; Lu et al. 2013; Malhotra et al. 2016; Kim et al. 2019; Fooladi et al. 2022; Garg et al. 2024; Singh and Seed 2024) providing a strong support to the present study. The gastro-intestinal system is the second most radiosensitive system of the body and contributes immensely to the lethality in irradiated mice. The average length of the villus, number of epithelial and goblet cells/villus was found to be decreased significantly ($p < 0.05\%$) with irradiated mice that were not pretreated with L-NAT (Figure 5c, e,g,h). However, in complete agreement with previous findings (Lu et al. 2013; Venkateswaran et al. 2019; Venkidesh et al. 2023), L-NAT pretreatment to irradiated mice, significantly protect the length of the villus, number of epithelial and goblet cells/villus (Figure 5d, e-h), suggested gastro-intestinal radioprotection ability of L-NAT in irradiated mice. Intestinal epithelial cells regeneration depends on intestinal crypt cell proliferation resulting in microvillus maintenance. Gamma radiation adversely affects intestinal crypt cells (Intestinal stem cells) and thus hampers their proliferation and survival, leading to intestinal denudation and mortality of the irradiated animals (Najafi et al. 2019). L-NAT pretreatment to irradiated mice was found highly effective in amelioration of radiation induced decrease of crypt number/villus, mitotic cells number/crypt, and number of goblet cells/crypt section in the jejunum section of small intestine (Figure 6d,e-h). To further verify the L-NAT mediated intestinal radioprotection, crypt stem cell marker's expression analysis was performed. Significant ($p < .05\%$) enhancement of Lgr-5, Bmi-1, Msi-1 and Dclk-1 marker's expression was evident with the intestinal tissue homogenate of irradiated mice that pretreated with L-NAT (Figure 7). These findings strongly suggested intestinal crypt stem cell protection activities of L-NAT in irradiated mice. Similar findings were also reported earlier (Bhanja et al. 2018; Sharma et al. 2020; Kenchegowda et al. 2023; Kwiatkowski et al. 2023) providing a gain support for the present investigation.

Due to continuous proliferation and high mitotic activities, seminiferous tubules are known as highly radiosensitive organs

of the male reproductive system. Gamma radiation exposure to the testicles leads to degeneration of spermatogonia and spermatocytes in seminiferous tubules (Kesari et al. 2018; Kaur et al. 2023), However, in the present study significant preservation of the number of spermatogonia-B and spermatocytes per seminiferous tubules were evident with irradiated mice that pretreated with L-NAT as compared to only irradiated mice that not pretreated with L-NAT (Figure 9c,d,h,g,k,l,o,p; Table 1). Recent reports (Haritwal et al. 2022; Yang et al. 2022) demonstrated similar radioprotection ability with other radioprotective agent in preclinical stage providing a strong support to the present investigation.

Radioprotective efficacy of L-NAT was also determined using a NHP model against gamma radiation whole body exposure (6.5 Gy; $LD_{70/40}$) (Burdelya et al. 2008). A significantly high (100%) rate of % survival was achieved with the irradiated NHPs (Male + Female) that were pretreated (-2h) with L-NAT (37.5 mg/kg, b.wt.) compared to irradiated NHPs (25% survival) that not pretreated with L-NAT (Figure 10). Hematology analysis demonstrated a significant recovery in blood parameters within day 14–30 (in both Male and Female animals) post irradiation periods (Figure 11a-g), suggesting bone marrow protection ability of L-NAT against gamma radiation induced hematopoietic system damage (Krivokrysenko et al. 2012). Several previous studies performed with NHP trial including IND status achieved molecule CBLB-502, B-300 and other advance stage radioprotective agents like tricotrinol, FSL-1 and indralin etc, also demonstrated bone marrow protection as the prime phenomenon that contributes to radioprotection in NHP model (Burdelya et al. 2008; Vasin et al. 2014; Singh et al. 2017; Garg et al. 2022; Singh et al. 2022; Brickey et al. 2023; Singh et al. 2024) and thus fully corroborated with the present investigation. To evaluate the radiation induced DNA damage in the blood cells of irradiated NHPs, alkaline comet assay was performed. Interestingly, significant reduction in comet tail was observed in the blood of irradiated NHPs that pretreated with L-NAT (Figure 14c,d). These findings suggest that L-NAT pretreatment may protect DNA against radiation-induced damage possibly *via* neutralizing free radicals resulting in reducing oxidative stress (Ravi et al. 2022; Darshana et al. 2023; Pratibha et al. 2023). Efficacy biomarker study demonstrated a dose depended (1-3X dose) increase in G-CSF and IL-6 along with down regulation of NFkB expression 2h after L-NAT administration to NHPs (Figure 15a,b,d). These findings suggested hematopoietic and immune system stimulatory along with anti-inflammatory activities of L-NAT that may contribute to radioprotection. Earlier identification and validation of G-CSF and IL-6 as efficacy biomarkers for radioprotective formulations of CBLB-502 and alpha tocopherol (Krivokrysenko et al. 2012; Singh et al. 2024; Wang et al. 2024) provided a strong support to the present investigation.

In conclusion, present study demonstrated radioprotective properties of L-NAT in rodent and NHP models. L-NAT provides significant whole body as well as systemic (hematopoietic, gastrointestinal and male reproductive system) protection against lethal doses of gamma radiation probably by antagonizing TRPV1 receptor and subsequently substance P release inhibition (Figure 16). However, further study to confirm L-NAT interaction with TRPV1 receptor and subsequent downstream signaling and its relevance with radioprotection need to be validated in future. Besides that, translational studies including L-NAT API synthesis, safety pharmacology in rodents, toxicity and pharmacokinetics studies in NHP models are underway and will be concluded before filing the IND dossier for human phase-I trial approval.

Acknowledgments

The authors gratefully acknowledge Director INMAS, for his administrative support. The authors also extend gratitude to Defence Research and Development Organisation, Ministry of Defence, Govt of India for financial support (Rakshak Project No. TD-15/INM313) for the present study. Authors also would like to acknowledge the Department of Biotechnology, Govt. of India for providing research fellowships to the research fellows involved in the present study.

Disclosure statement

No potential conflict of interest was reported by the author(s).

Funding

This research received specific grant from Defence Research and Development Organization (DRDO), Ministry of Defense Government of India.

Notes on contributors

Raj Kumar, is a senior scientist and head Department of Radiation Biotechnology, Institute of Nuclear Medicine and Allied Sciences, Delhi, India. His research focuses on the development of radiation countermeasures especially radioprotector since last 25 years for medical management of radiation injuries.

Pratibha Kumari, is a postgraduate researcher in the Department of Radiation Biotechnology, Institute of Nuclear Medicine and Allied Sciences, Delhi, India. Her prime focuses on the evaluation of gamma radiation effects on gastrointestinal system.

Neelanshu Gaurav, is a postgraduate researcher in the Department of Radiation Biotechnology, Institute of Nuclear Medicine and Allied Sciences, Delhi, India. His prime focuses on the evaluation of gamma radiation's effects on DNA damages and its repair. He also focuses on molecular docking and other bioinformatics studies.

Ravi Kumar, is a postgraduate researcher in the Department of Radiation Biotechnology, Institute of Nuclear Medicine and Allied Sciences, Delhi, India. His prime focuses on the evaluation of gamma radiation effects on CNS and neuronal cells.

Darshana Singh is a postgraduate researcher in the Department of Radiation Biotechnology, Institute of Nuclear Medicine and Allied Sciences, Delhi, India. Her prime focuses on the radioprotection of the hematopoietic system.

Poonam Malhotra, is a postgraduate researcher in the Department of Radiation Biotechnology, Institute of Nuclear Medicine and Allied Sciences, Delhi, India. Her prime focuses on the radioprotection of hematopoietic system using macrophages as a model system.

Shravan Kumar Singh, , is a senior scientist in the Department of Radiation Biotechnology, Institute of Nuclear Medicine and Allied Sciences, Delhi, India. His research focuses on the development of radiation biomarkers and bioinformatics studies.

Ravi Shankar Bhatta, is a senior scientist in the Department of pharmaceutics, Central Drug Research Institute Lucknow, India. He is a known expert in the area of formulation development, pharmacokinetics, and toxicity evaluation in rodents and primate models.

Anil Kumar, is a senior scientist at the National Institute of Immunology, Delhi, India. His prime focuses on immunological studies in primate model and radiation induced carcinogensis.

Perumal Nagarajan, is a senior scientist and principle veterinarian at National Institute of Immunology, Delhi, India. His prime focuses on immunological studies in rodents and primate model.

Surender Singh, is a senior scientist and principle veterinarian at National Institute of Immunology, Delhi, India. His prime focuses on immunological studies in rodents and primate model especially histopathological and hematological analysis.

Nishu Dalal, is a postgraduate researcher at National Institute of Immunology, Delhi, India. Her prime focuses on metabomic and proteomic studies on rodents primate model.

Bal Gangadhar Roy, is a senior scientist and principal veterinarian at Institute of Nuclear Medicine and Allied Sciences, Delhi, India. His prime focuses on biochemistry, immunology of radiation-exposed rodents.

Anant Narayan Bhatt, is a senior scientist and head department of Radiation Biotechnology, Institute of Nuclear Medicine and Allied Sciences, Delhi, India. His research focuses on the development of radiation countermeasures.

Sudhir Chandna, is a senior scientist and director of Institute of Nuclear Medicine and Allied Sciences, Delhi, India. His research focuses on the development of radiation countermeasure, radiation biomarkers and radiation Biodosimetry and cytogentics studies on radiation exposed animals and cellular system.

ORCID

Raj Kumar http://orcid.org/0000-0002-9702-2788

Data availability statement

The authors confirm that the data supporting the findings of the present study are available on request.

References

Abdi GN, Abedi R, Ebrahimnejad GK, Khosravanipour M, Moradi S, Banaei A, Astani A, Najafi M, Zare MH, Farhood B. 2018. Estimation of radiation dose-reduction factor for cerium oxide nanoparticles in MRC-5 human lung fibroblastic cells and MCF-7 breast-cancer cells. Artificial Cells, Nanomed. Biotech. 46(sup3):1215–1225. doi:10.1080/21691401.2018.1536062.

Abe N, Jobu K, Yokota J, Yoshioka S, Miyamura M, Hyodo M. 2013. TRPV1 agonist increases the amount of substance P in Saliva. Japan Pharmacol. Therap. 41(7):669–675.

Azmoonfar R, Khosravi H, Rafieemehr H, Mirzaei F, Dastan D, Ghiasvand MR, Khorshidi L, Pashaki AS. 2023. Radioprotective effect of Malva sylvestris L. against radiation-induced liver, kidney and intestine damages in rat: a histopathological study. Biochem. Biophys. Rep. 34:101455. doi:10.1016/j.bbrep.2023.101455.

Bhanja P, Norris A, Gupta-Saraf P, Hoover A, Saha S. 2018. BCN057 induces intestinal stem cell repair and mitigates radiation-induced intestinal injury. Stem Cell Res. Therapy. 9:1–15.

Bode AM, Cho Y-Y, Zheng D, Zhu F, Ericson ME, Ma W-Y, Yao K, Dong Z. 2009. 2009. Transient receptor potential type vanilloid 1 suppresses skin carcinogenesis. Cancer Res. 69(3):905–913. doi:10.1158/0008-5472.CAN-08-3263.

Bowden JJ, Garland AM, Baluk P, Lefevre P, Grady EF, Vigna SR, Bunnett NW, McDonald DM. 1994. Direct observation of substance P-induced internalization of neurokinin 1 (NK1) receptors at sites of inflammation. Proc Natl Acad Sci USA. 91(19):8964–8968. doi:10.1073/pnas.91.19.8964.

Brickey WJ, Caudell DL, Macintyre AN, Olson JD, Dai Y, Li S, Dugan GO, Bourland JD, O'Donell LM, Tooze JA, et al. 2023. The TLR2/TLR6 ligand FSL-1 mitigates radiation-induced hematopoietic injury in mice and nonhuman primates. Proc Natl Acad Sci. 120(50):e2122178120. doi:10.1073/pnas.2122178120.

Burdelya LG, Gleiberman AS, Toshkov I, Aygun-Sunar S, Bapardekar M, Manderscheid-Kern P, Bellnier D, Krivokrysenko VI, Feinstein E, Gudkov AV. 2012. Toll-like receptor 5 agonist protects mice from dermatitis and oral mucositis caused by local radiation: implications for head-and-neck cancer radiotherapy. Int. J. Rad. Onco. Biol. Phys. 83(1), 228–234.

Burdelya L G, Krivokrysenko VI, Tallant TC, Strom E, Gleiberman AS, Gupta D, Kurnasov OV, Fort FL, Osterman AL, DiDonato JA, Feinstein, Gudkov AV. 2008. An agonist of toll-like receptor 5 has radioprotective activity in mouse and primate models. Science, 320(5873), 226–230.

Clement JJ, Johnson RK. 1982. Influence of WR 2721 on the efficacy of radiotherapy and chemotherapy of murine tumors. Int. J. Rad. Onco. Biol. Phys. 8(3–4), 539–542.

Darshana S, Malhotra P, Agarwal P, Kumar R. 2023. N-acetyl-l-tryptophan (NAT) ameliorates radiation-induced cell death in murinemacrophages J774A.1 via regulating redox homeostasis and mitochondrialdysfunction. J. Biochem. Mol. Toxicol. 38(1), e2359. doi:10.1002/jbt.23529.

de Jong PR, Takahashi N, Harris AR, Lee J, Bertin S, Jeffries J, Jung M, Duong J, Triano AI, Lee J, et al. 2014. Ion channel TRPV1- dependent activation of PTP1B suppresses EGFR-associated intestinal tumorigenesis. J Clin Invest. 124(9):3793–3806. doi:10.1172/JCI72340.

Fonseca BM, Correia-da-Silva G, Teixeira NA. 2018. Cannabinoid-induced cell death in endometrial cancer cells: involvement of TRPV1 receptors in apoptosis. J Physiol Biochem; 74: 261–272.

Fooladi M, Cheki M, Shirazi A, Sheikhzadeh, P., Amirrashedi M, Ghahramani F, Khoobi M. 2022. Histopathological evaluation of protective effect of telmisartan against radiation-induced bone marrow injury. J. Biomed. Phys. Engin. 12(2): 277–284. doi:10.31661/jbpe.v0i0.2012-1243

Garg TK, Garg S, Miousse IR, Wise SY, Carpenter AD, Fatanmi OO, van Rhee F, Singh VK, Hauer-Jensen M. 2022. Gamma-tocotrienol modulates total-body irradiation-induced hematopoietic injury in a nonhuman primate model. IJMS. 23(24):16170. doi:10.3390/ijms232416170.

Garg TK, Garg S, Miousse IR, Wise SY, Carpenter AD, Fatanmi OO, Rhee FV, Singh VK, Hauer-Jensen M. 2024. Modulation of Hematopoietic Injury by a Promising Radioprotector, Gamma-Tocotrienol, in Rhesus Macaques Exposed to Partial-Body Radiation. Rad. Res. 201(1):55–70.

Gazzieri D, Trevisani M, Springer J, Harrison S, Cottrell GS, Andre E, Nicoletti P, Massi D, Zecchi S, Nosi D, et al. 2007. Substance P released by TRPV1-expressing neurons produces reactive oxygen species that mediate ethanol-induced gastric injury. Free Radic Biol Med. 43(4):581–589. doi:10.1016/j.freeradbiomed.2007.05.018.

Ghosh SP, Perkins MW, Hieber K, Kulkarni S, Kao TC, Reddy EP, Reddy MVR, Maniar M, Seed T, Kumar KS. 2009. Radiation protection by a new chemical entity, Ex-Rad™: Efficacy and mechanisms. Rad.Res. 171(2):173–179. doi:10.1667/RR1367.1.

Grace MB, Singh VK, Rhee JG, Jackson IWE, Kao TC, Whitnall MH. 2012. 5-AED enhances survival of irradiated mice in a G-CSF-dependent manner, stimulates innate immune cell function, reduces radiation-induced DNA damage and induces genes that modulate cell cycle progression and apoptosis. J. Rad. Res. 53(6):840–853. doi:10.1093/jrr/rrs060.

Gouin O, L'Herondelle K, Lebonvallet N, Gall-Ianotto CL, Sakka M, Buhé V, Plée-Gautier E, Carré JL, Lefeuvre L, Misery L, et al. 2017. TRPV1 and TRPA1 in cutaneous neurogenic and chronic inflammation: pro-inflammatory response induced by their activation and their sensitization. Protein Cell. 8(9):644–661. doi:10.1007/s13238-017-0395-5.

Guan B, Li D, Meng A. 2023. Development of radiation countermeasure agents for acute radiation syndromes. Animal Model Exp Med. 6(4):329–336. doi:10.1002/ame2.12339.

Haritwal T, Kalra N, Agrawala PK. 2022. Mitigation of radiation injury to reproductive system of male mice by Trichostatin A. Mutat Res Genet Toxicol Environ Mutagen. 881:503522. doi:10.1016/j.mrgentox.2022.503522.

Huang J, Liu J, Qiu L. 2020. Transient receptor potential vanilloid 1 promotes EGFR ubiquitination and modulates EGFR/MAPK signaling in pancreatic cancer cells. Cell Biochem. Funct. 38(4):401–408. doi:10.1002/cbf.3483.

Kang AD, Cosenza SC, Bonagura M, Manair M, Reddy MVR, Reddy EP. 2013. ON01210. Na (Ex-RAD®) mitigates radiation damage through activation of the AKT pathway. PLoS One. 8(3):e58355. doi:10.1371/journal.pone.0058355.

Kaur P, Rai U, Singh R. 2023. Genotoxic Risks to Male Reproductive Health from Radiofrequency Radiation. Cells. 12(4):594. doi:10.3390/cells12040594.

Kenchegowda D, Bolduc DL, Kurada L, Blakely WF. 2023. Severity scoring systems for radiation-induced GI injury-Prioritization for use of GI-ARS medical countermeasures. Int J Radiat Biol. 99(7):1037–1045. doi:10.1080/09553002.2023.2210669.

Kesari KK, Agarwal A, Henkel R. 2018. Radiations and male fertility. Reprod Biol Endocrinol. 16(1):118. doi:10.1186/s12958-018-0431-1.

Kim JY, Park JH, Seo SM, Park JI, Jeon HY, Lee HK, Yoo RJ, Lee YJ, Woo SK, Lee WJ, et al. 2019. Radioprotective effect of newly synthesized toll-like receptor 5 agonist, KMRC011, in mice exposed to total-body irradiation. J. Rad. Res. 60(4):432–441. doi:10.1093/jrr/rrz024.

Krivokrysenko VI, Shakhov AN, Singh VK, Bone F, Kononov Y, Shyshynova I, Cheney A, Maitra RK, Purmal A, Whitnall MH, et al. 2012. Identification of granulocyte colony-stimulating factor and interleukin-6 as candidate biomarkers of CBLB502 efficacy as a medical radiation countermeasure. J Pharmacol Exp Ther. 343(2):497–508. doi:10.1124/jpet.112.196071.

Kwiatkowski E, Suman S, Kallakury BV, Datta K, Fornace AJ, Jr, Kumar S. 2023. Expression of Stem Cell Markers in High-LET Space Radiation-Induced Intestinal Tumors in Apc 1638N/+ Mouse Intestine. Cancers (Basel). 15(17):4240. doi:10.3390/cancers15174240.

Landauer MR, Harvey AJ, Kaytor MD, Day RM. 2019. Mechanism and therapeutic window of a genistein nanosuspension to protect against hematopoietic-acute radiation syndrome. J. Rad. Res. 60(3):308–317. doi:10.1093/jrr/rrz014.

Lehnig M, Kirsch M, Lehnig M, Kirsch M. 2007. 15N-CIDNP investigations during tryptophan, N-acetyl-L-tryptophan, and melatonin nitration with reactive nitrogen species. Free Rad. Res. 41(5):523–535. doi:10.1080/10715760601161445.

Li F, Yang W, Jiang H, Guo C, Huang AJW, Hu H, Liu Q. 2019. TRPV1 activity and substance P release are required for corneal cold nociception. Nat Commun. 10(1):5678. doi:10.1038/s41467-019-13536-0.

Li L, Cheng CC, Chengyao CC, Tian Xiao T, Yangchao Chen Y, Yongxiang Zhao Y, Duo Zheng D. 2021. The Impact of TRPV1 on Cancer Pathogenesis and Therapy: A Systematic Review. Int J Biol Sci. 17(8):2034–2049. doi:10.7150/ijbs.59918.

Li W, Fotinos A, Wu Q, Chen Y, Zhu Y, Baranov S, Tu Y, Zhou EW, Sinha B, Kristal BS, et al. 2015. N-acetyl Ltryptophan N-acetyl-L-tryptophan delays disease onset and extends survival in an amyotrophic lateral sclerosis transgenic mouse model. Neurobiol. Disease. 80:93–103. doi:10.1016/j.nbd.2015.05.002.

Liu Y, Miao L, Guo Y, Tian H. 2021. Preclinical evaluation of safety, pharmacokinetics, efficacy, and mechanism of radioprotective agent HL-003. Oxid. Med. Cellul. Longe. 2021(1):6683836. doi:10.1155/2021/6683836.

Lu X, Nurmemet D, Bolduc DL, Elliott TB, Kiang JG. 2013. Radioprotective effects of oral 17-dimethylaminoethylamino-17-demethoxygeldanamycin in mice: bone marrow and small intestine. Cell Biosci. 3(1):36. doi:10.1186/2045-3701-3-36.

Lu Y, Hu M, Zhang Z, Qi Y, Wang J. 2020. The regulation of hematopoietic stem cell fate in the context of radiation. Rad. Med. Protec. 1(1):31–34. doi:10.1016/j.radmp.2020.01.002.

Malhotra P, Kumar R. 2016. N acetyl tryptophan glucopyranoside (NATG) as a countermeasure against radiation-induced immunosuppression in murine macrophages J774A.1 cells. Free Rad. Res. 50(11):1265–1278.

Malhotra P, Adhikari M, Singh SK, Kumar R. 2015. N-acetyl tryptophan glucopyranoside (NATG) provides radioprotection to murine macrophages J774A.1 cells. Free Rad. Res. 49(12):1488–1498. doi:10.3109/10715762.2015.1095295.

Malhotra P, Gupta AK, Singh D, Mishra S, Singh SK, Kumar R. 2018. N-Acetyl-tryptophan glucoside (NATG) protects J774A.1 murine macrophages against gamma radiation-induced cell death by modulating oxidative stress. Mol Cell Biochem. 447(1-2):9–19. doi:10.1007/s11010-018-3289-9.

Malhotra P, Gupta AK, Singh D, Mishra S, Singh SK, Kumar R. 2019. Protection to immune system of mice by N-acetyl tryptophan glucoside (NATG) against gamma radiation induced immune suppression. Mol Immunol. 114:578–590. doi:10.1016/j.molimm.2019.09.003.

Masumoto K, Tsukimoto M, Kojima S. 2013. Role of TRPM2 and TRPV1 cation channels in cellular responses to radiation-induced DNA damage. Biochim Biophys Acta. 1830(6):3382–3390. doi:10.1016/j.bbagen.2013.02.020.

Meza-León B, Gratzinger D, Aguilar-Navarro AG, Juárez-Aguilar FG, Rebel VI, Torlakovic E, Purton LE, Dorantes-Acosta EM, Escobar-Sánchez A, Dick JE, et al. 2021. Human, mouse, and dog bone marrow show similar mesenchymal stromal cells within a distinctive microenvironment. Exp Hematol. 100:41–51. doi:10.1016/j.exphem.2021.06.006.

Mun GI, Kim S, Choi E, Kim CS, Lee YS. 2018. Pharmacology of natural radioprotectors. Arch Pharm Res. 41(11):1033–1050. doi:10.1007/s12272-018-1083-6.

Nair AB, Jacob S. 2016. A simple practice guide for dose conversion between animals and human. J Basic Clin Pharm. 7(2):27–31. doi:10.4103/0976-0105.177703.

Najafi M, Cheki M, Hassanzadeh G, Amini P, Shabeeb D, Musa AE. 2019. The radioprotective effect of combination of melatonin and metformin on rat duodenum damage induced by ionizing radiation: A histological study. Adv Biomed Res. 8(51)8:51. :51. doi:10.4103/abr.abr_68_19.

Nicholas D. 2002. Hematologic consequences of exposure to ionizing radiation. Exp. Hematol. 30:513–528.

Obrador E, Salvador R, Villaescusa JI, Soriano JM, Estrela JM, Montoro A. 2020. Radioprotection and radiomitigation: from the bench to clinical practice. Biomedicines. 8(11):461. doi:10.3390/biomedicines8110461.

Okada Y, Reinach PS, Shirai K, Kitano A, Kao WW, Flanders KC, Masayasu M, Liu H, Zhang J, Saika S. 2011. TRPV1 involvement in inflammatory tissue fibrosis in mice. Am J Pathol. 178(6):2654–2664. doi:10.1016/j.ajpath.2011.02.043.

Pecze L, Blum W, Henzi T, Schwaller B. 2016. Endogenous TRPV1 stimulation leads to the activation of the inositol phospholipid pathway necessary for sustained Ca(2+) oscillations. Biochim Biophys Acta. 1863(12):2905–2915. doi:10.1016/j.bbamcr.2016.09.013.

Pratibha K, Ravi K, Singh D, Kumar R. 2023. N-acetyl-L-tryptophan (NAT) provides protection tointestinal epithelial cells (IEC-6) against radiation-induced apoptosis via modulation of oxidative stress and mitochondrial membrane integrity. Mol Biol Rep. 50(8):6381–6397. doi:10.1007/s11033-023-08579-y.

Ravi K, Pratibha K, Pandey S, Singh SK, Kumar R. 2022. Amelioration of Radiation-Induced Cell Death in Neuro2a Cells by Neutralizing Oxidative Stress and Reducing Mitochondrial Dysfunction Using N-Acetyl-L-Tryptophan. Oxid. Med. Cellul. Longe. 20222022::1–22. doi:10.1155/2022/9124365.

Satyamitra MM, Kulkarni S, Ghosh SP, Mullaney CP, Condliffe D, Srinivasan V. 2011. Hematopoietic recovery and amelioration of radiation-induced lethality by the vitamin E isoform δ-tocotrienol. Radiat Res. 175(6):736–745. doi:10.1667/RR2460.1.

Sharma A, Akagi K, Pattavina B, Wilson KA, Nelson C, Watson M, Maksoud E, Harata A, Ortega M, Brem RB, et al. 2020. Musashi expression in intestinal stem cells attenuates radiation-induced decline in intestinal permeability and survival in Drosophila. Scientific Rep. 10(1):1–16. doi:10.1038/s41598-020-75867-z.

Sharma V, McNeill JH. 2009. To scale or not to scale: the principles of dose extrapolation. Br J Pharmacol. 157(6):907–921. doi:10.1111/j.1476-5381.2009.00267.x.

Singh PK, Krishnan S. 2015. Vitamin E analogs as radiation response modifiers. Evid Based Complement Alternat Med. 2015:741301–741316. doi:10.1155/2015/741301.

Singh VK, Beattie LA, Seed TM. 2013. Vitamin E: tocopherols and tocotrienols as potential radiation countermeasures. J Radiat Res. 54(6):973–988. doi:10.1093/jrr/rrt048.

Singh VK, Fatanmi OO, Wise SY, Carpenter AD, Olsen CH. 2022. Determination of lethality curve for cobalt-60 gamma-radiation source in rhesus macaques using subject-based supportive care. Rad. Res. 198(6):599–614.

Singh VK, Newman VL, Romaine PL, Wise SY, Seed TM. 2014. Radiation countermeasure agents: an update (2011–2014). Expert. opin. Therape. Patents. 24(11):1229–1255. doi:10.1517/13543776.2014.964684.

Singh VK, Romaine PL, Seed TM. 2015. Medical countermeasures for radiation exposure and related injuries: characterization of medicines, FDA-approval status and inclusion into the strategic national stockpile. Health Phys. 108(6):607–630. doi:10.1097/HP.0000000000000279.

Singh VK, Seed TM. 2024. The potential value of 5-androstenediol in countering acute radiation syndrome. Drug Discov Today. 29(2):103856. doi:10.1016/j.drudis.2023.103856.

Singh VK, Serebrenik AA, Wise SY, Petrus SA, Fatanmi OO, Kaytor MD. 2024. BIO-300: A Prophylactic Radiation Countermeasure for Acute Radiation Syndrome. Mil Med. 189(Suppl 3):390–398. doi:10.1093/milmed/usae156.

Singh VK, Wise SY, Scott JR, Romaine PLP, Victoria L, Newman VL, Fatanmi OO. 2024. Radioprotective efficacy of delta-tocotrienol, a vitamin E isoform, is mediated through granulocyte colony-stimulating factor. Life Sci. 16(704):14966. doi:10.1016/j.bbrc.2024.149661.

Singh VK, Garcia M, Seed TM. 2017. A review of radiation countermeasures focusing on injury- specific medicinals and regulatory approval status: part II. Countermeasures for limited indications, internalized radionuclides, emesis, late effects, and agents demonstrating efficacy in large animals with or without IND status. Int J Radiat Biol. 93(9):870–884. doi:10.1080/09553002.2017.1338782.

Singh VK, Srinivasan V, Toles R, Karikari P, Seed T, Papas KA, Hyatt JA, Kumar KS. 2005. Radiation protection by the antioxidant alpha-tocopherol succinate. Radiation Bioeffects and Countermeasures. Human Factors and Medicine Panel Research Task Group 099 "Radiation Bioeffects and Countermeasures" meeting, held in Bethesda, Maryland, USA, June 21-23, 2005, and published in AFRRI CD 05-2.

Tang HB, Yu-Sang Li YS, Koji Arihiro K, Yoshihiro Nakata Y. 2007. Activation of the Neurokinin-1 Receptor by Substance P Triggers the Release of Substance P from Cultured Adult Rat Dorsal Root Ganglion Neurons. Mol Pain. 3:42. doi:10.1186/1744-8069-3-42.

Teodoro FC, Tronco Júnior MF, Aleksander R, Zampronio AR, Alessandra C, Martini AC, Giles A. Rae GA, Juliana G. Chichorro JG. 2013. Peripheral substance P and neurokinin-1 receptors have a role in inflammatory and neuropathic orofacial pain models. Neuropeptides. 47(3):199–206. doi:10.1016/j.npep.2012.10.005.

Travlos GS. 2006. Histopathology of bone marrow. Toxicol Pathol. 34(5):566–598. doi:10.1080/01926230600964706.

Vasin MV, Semenov LF, Suvorov NN, Antipov VV, Ushakov IB, Ilyin LA, Lapin BA. 2014. Protective effect and the therapeutic index of indralin in juvenile rhesus Macaque. J Radiat Res. 55(6):1048–1055. doi:10.1093/jrr/rru046.

Venkateswaran K, Shrivastava A, Agrawala PK, Prasad AK, Devi SC, Manda K, Parmar VS, Dwarakanath BS. 2019. Mitigation of radiation-induced gastro-intestinal injury by the polyphenolic acetate 7, 8-diacetoxy-4-methylthiocoumarin in mice. Sci Rep. 9(1):14134. doi:10.1038/s41598-019-50785-x.

Venkidesh BS, Shankar SR, Narasimhamurthy RK, Rao SBS, Mumbrekar KD. 2023. Radioprotective potential of probiotics against gastrointestinal and neuronal toxicity: a preclinical study. Clin Transl Oncol. 25(11):3165–3173. doi:10.1007/s12094-023-03184-8.

Vinuesa AG, Sancho R, García-Limones C, Behrens A, ten Dijke P, Calzado MA, Muñoz E. 2012. Vanilloid receptor-1 regulates neurogenic inflammation in colon and protects mice from colon cancer. Cancer Res. 72(7):1705–1716. doi:10.1158/0008-5472.CAN-11-3693.

Wang S, Zuo Z, Ouyang Z, Liu X, Wang J, Shan Y, Meng R, Zhao Z, Liu X, Liu X, et al. 2024. Sequential administration of delta- tocotrienol ameliorates radiation-induced myelosuppression in mice and non-human primates through inducing G-CSF production. Biochem Biophys Res Commun. 704:149661. 16 doi:10.1016/j.bbrc.2024.149661.

Waning J, Vriens J, Owsianik G, Stüwe L, Mally S, Fabian A, Frippiat C, Nilius B, Schwab A. 2007. A novel function of capsaicin-sensitive TRPV1 channels: involvement in cell migration. Cell Calcium. 42(1):17–25. doi:10.1016/j.ceca.2006.11.005.

Wickramasinghe JS, Udagama PV, Dissanayaka VH, Weerasooriya AD, Goonasekera HW. 2022. Plant based radioprotectors as an adjunct to radiotherapy: advantages and limitations. J Radiol Prot. 42(2):021001. doi:10.1088/1361-6498/ac5295.

Wu TT, Peters AA, Tan PT, Roberts-Thomson SJ, Monteith GR. 2014. Consequences of activating the calcium-permeable ion channel TRPV1 in breast cancer cells with regulated TRPV1 expression. Cell Calcium. 56(2):59–67. doi:10.1016/j.ceca.2014.04.006.

Yan KS, Chia LA, Li X, Ootani A, Su J, Lee JY, Su N, Luo Y, Heilshorn SC, Amieva MR, et al. 2012. The intestinal stem cell markers Bmi1 and Lgr5 identify two functionally distinct populations. Proc Natl Acad Sci U S A. 109(2):466–471. doi:10.1073/pnas.1118857109.

Yang J, Xu R, Luan Y, Fan H, Yang S, Liu J, Zeng H, Shao L. 2022. Rapamycin ameliorates radiation-induced testis damage in mice. Front Cell Dev Biol. 10:783884. doi:10.3389/fcell.2022.783884.

Yang Y, Guo W, Ma J, Xu P, Zhang W, Guo S, Liu L, Ma J, Shi Q, Jian Z, et al. 2018. Downregulated TRPV1 Expression Contributes to Melanoma Growth via the Calcineurin-ATF3-p53 Pathway. J Invest Dermatol. 138(10):2205–2215. doi:10.1016/j.jid.2018.03.1510.